 doi:10.20944/preprints202204.0017.v1

Article

Improving fuel properties and hydrocarbon content from residual fat pyrolysis vapors over activated red mud pellets in two-stage reactor: Optimization of reaction time and catalyst content

Caio Campos Ferreira[1], Lucas Pinto Bernar[1], Augusto Fernando de Freitas Costa[1], Haroldo Jorge da Silva Ribeiro[1], Nathalia Lobato Moraes[2], Yasmin Santos Costa[2], Ana Cláudia Fonseca Bahia[2], Sílvio Alex Pereira da Mota[3], Fernanda Paula da Costa Assunção[4], Carlos Castro Vieira Quaresma[5], Douglas Alberto Rocha de Castro[5], Marcelo Costa Santos[1], Neyson Martins Mendonça[2], Sergio Duvoisin Jr.[6], Luiz Eduardo Pizarro Borges[7] and Nélio Teixeira Machado[1,2]*

[1] Graduate Program of Natural Resources Engineering of Amazon, Campus Profissional-UFPA, Universidade Federal do Pará, Rua Augusto Corrêa N° 1, Belém 66075-110, Brazil; caiocf7@hotmail.com (C.C.F.); lucas.bernar7@gmail.com (L.P.B.); affreitas@ufpa.br (A.F.d.F.C.); ribeiroengq@hotmail.com (H.J.d.S.R.); marcelo.santos@ufra.edu.br (M.C.S.)

[2] Faculty of Sanitary and Environmental Engineering, Campus Profissional-UFPA, Universidade Federal do Pará, Rua Corrêa N° 1, Belém 66075-900, Brazil; nathalia.morraes@icb.ufpa.br (N.L.M.); yasmincosta.eng@hotmail.com (Y.S.C.); anaclaudia.fonsecabaia@yahoo.com (A.C.F.B.); neysonmm@ufpa.br (N.M.M.)

[3] Graduate Program of Chemistry, Universidade Federal do Sul e Sudeste do Pará, Folha 31, Quadra 7, Lote Especial - Nova Marabá, CEP: 68.507.590, Marabá/PA, Brasil, silviomota@unifesspa.edu.br (S.A.P.d.M.)

[4] Graduate Program of Civil Engineering, Campus Profissional-UFPA, Universidade Federal do Pará, Rua Augusto Corrêa N° 1, Belém 66075-110, Brazil; fernanda.assuncao.itec@gmail.com (F.P.d.C.A.)

[5] Centro Universitário Luterano de Manaus – CEULM/ULBRA, Avenida Carlos Drummond de Andrade N°. 1460, Manaus 69077-730, Brazil; douglascastro87@hotmail.com (D.A.R.d.C.); carlos.castrovq@gmail.com (C.C.V.Q.)

[6] Faculty of Chemical Engineering, Universidade do Estado do Amazonas-UEA, Avenida Darcy Vargas N°. 1200, Manaus 69050-020, Brazil; sjunior@uea.edu.br (S.D.Jr.)

[7] Laboratory of Catalyst Preparation and Catalytic Cracking, Section of Chemical Engineering, Instituto Militar de Engenharia-IME, Praça General Tibúrcio N°. 80, Rio de Janeiro 22290-270, Brazil; luiz@ime.eb.br (L.E.P.B.)

* Correspondence: machado@ufpa.br; Tel.: +55-91-984-620-325

Abstract: This work aims to investigate the effect of catalyst content and reaction time by catalytic upgrading from pyrolysis vapors of residual fat at 450 °C and 1.0 atmosphere, on the yields of reaction products, physicochemical properties (density, kinematic viscosity, refractive index, and acid value) and chemical composition of organic liquid products (OLP), over a catalyst fixed bed reactor, in semi pilot scale. Pellets of Red Mud chemically activated with 1.0 M HCl were used as catalysts. The experiments were carried out at 450 °C and 1.0 atmosphere, using a process schema consisting of a thermal cracking reactor of 2.0 L coupled to a catalyst fixed bed reactor of 53 mL, without catalyst and using 5.0, 7.5, and 10.0% (wt.) Red Mud pellets activated with 1.0 M HCl, in batch mode. Samples of liquid phase products were withdrawn during the course of reaction at 40, 50, 60, 70 and 80 min in order to analyze the process kinetics. The physicochemical properties (density, kinematic viscosity, acid value, and refractive index) of OLP were determined by official methods. The chemical functions present in OLP determined by FT-IR and the chemical composition by GC-MS. The thermal catalytic cracking of residual fat show OLP yields from 54.4 to 84.88 (wt.%), aqueous phase yields between 2.21 and 2.80 (wt.%), solid phase yields (coke) between 1.30 and 8.60 (wt.%), and gas yields from 11.61 to 34.22

 doi:10.20944/preprints202204.0017.v1

(wt.%). The yields of OLP increases with increasing catalyst content while those of aqueous, gaseous and solid phase decreases. For all the thermal and thermal catalytic cracking experiments, the density, kinematic viscosity, and acid value of OLP decreases with increasing reaction time. The GC-MS of liquid reaction products identified the presence of hydrocarbons (alkanes, alkenes, cycloalkanes, and aromatics) and oxygenates (carboxylic acids, ketones, esters, alcohols, and aldehydes). For all the thermal and thermal catalytic cracking experiments, the hydrocarbon content within OLP increases with reaction time, while those of oxygenates decrease, reaching concentrations of hydrocarbons up to 95.35% (area.). The best results for the physicochemical properties (density, kinematic viscosity, and acid value) and the maximum hydrocarbon content of OLP were obtained at 450 °C and 1.0 atmosphere, using a catalyst fixed bed reactor, with 5.0% (wt.) Red Mud pellets activated with 1.0 M HCl as catalyst.

Keywords: Residual fat; Red Mud; Chemical activation; Thermal catalytic cracking; Fixed bed reactor, Liquid hydrocarbons.

1. Introduction

Catalytic upgrading of coal and biomass pyrolysis volatiles and/or vapors is one of the most potential processes to improve the quality of bio-oils not only by converting volatiles substances into valuable chemicals, particularly light aromatic hydrocarbons, but also making it possible to get better the transport (kinematic viscosity) and physical-chemistry properties (acidity, corrosivity, oxidative stability, etc.) of bio-oils, and the literature reports several studies on the subject [1-34].

Most studies on catalytic upgrade focused on the pyrolysis volatiles/vapors of *lignocelullosic biomass* including poplar wood [1], Walnut shell [7], rape straw [8, 12, 16, 19], Yunnan pine [10], rice husk [13], beech wood [14, 18], Canadian white pine wood-ships [17], Southern yellow pine [21-22], lignocellulosic material [24], sugarcane bagasse [25], alkali lignin [28], corn Stover [29], cellulose [30, 34], lignin [30], Pine sawdust [31], pyrolysis volatiles of *coal/lignite* including Pingshuo bituminous coal [2, 32], Baiyinhua lignite [3, 11], Shengli lignite [4, 6], Fenxi bituminous coal [5], Bai Yinhua lignite [23], Shendong long-flame coal [23], Xinwen gas coal [23], Luliang coking coal [23], Anyang anthracite coal [23], Fucheng coal [32], Hexi coal [32], pyrolysis volatiles/vapors of *lipid-base materials* including castor seed oil [9], Jatropha waste [15], und until pyrolysis volatiles/vapors of monosaccharides (glucose) [30], and waste tires granules [26].

The state of art, progress, and new trends on catalytic upgrading of pyrolysis volatiles from coal, biomass, lipid-material, and other materials (glucose, waste tires granules, etc.) were described in details on the excellent reviews of *Ren et al.* [20], Nishu *et. al.* [27], and Asadieraghi *et. al*. [33].

Among the various catalysts applied by the catalytic upgrade of pyrolysis volatiles from coal, biomass, lipid-material, and other materials (glucose, waste tires granules, etc.), the most used were HZSM-5 [2-4, 6-8, 10-12, 15-16, 19, 23, 25, 30-31], ZSM-5 [10, 13-14, 16, 22, 26, 28-29, 34], Y-zeolite [5, 26, 32], β-zeolite [21], faujasite-zeolite [17], mesoporous aluminosilicates [18], clay mineral (Kaolin) [9], as well as oxide-base catalysts [1, 9, 14, 24], including titania and zirconia/titania based catalysts (TiO_2-Rutile, TiO_2-Anatase, ZrO_2/TiO_2, Ce/TiO_2-Rutile, Ru-Ce/TiO_2-Rutile, Pd-Ce/TiO_2-Rutile, Ce/TiO_2-Anatase, Ru-Ce/TiO_2-Anatase, Pd-Ce/TiO_2-Anatase, Ce/ZrO_2/TiO_2, Ru-Ce/ZrO_2/TiO_2, Pd-Ce/ZrO_2/TiO_2) [1], HZSM-5 and Mo-modified HZSM-5 (HZSM-5, Mo/HZSM-5) [2], mono/bimetal loaded mesoporous HZSM-5 (HZSM-5, Co/HZSM-5, Mo-Co/HZSM-5, Ni-

Co/HZSM-5, NaOH-HZSM-5, Co/NaOH-HZSM-5, Mo-Co/NaOH-HZSM-5, Ni-Co/NaOH-HZSM-5) [3], metal-loaded HZSM-5 (HZSM-5, Co/HZSM-5, Mo/HZSM-5, Ni/HZSM-5) [4], Y-zeolite (USY, SBA-15, Al/SBA-15) [5], HZSM-5 based sulfated zirconium (HZSM-5, $AT_{0.2}$/HZSM-5, $AT_{0.2}/SZ_{2:1}$HZSM-5, $AT_{0.2}/SZ_{4:1}$HZSM-5, $AT_{0.2}/SZ_{6:1}$HZSM-5, $AT_{0.2}/SZ_{8:1}$HZSM-5) [6], Co-Ni modified ZSM-5 zeolite (HZSM-5, 5%-Co-HZSM-5, 5%-Ni-HZSM-5, SBA-15, 5%-Al/SBA-15, 10%-Al/SBA-15, 30%-Fe/SBA-15, 50%-Fe/SBA-15) [7], nanocrystalline HZSM-5 (Al/Si=25/HZSM-5, Al/Si=50/HZSM-5, Al/Si=75/HZSM-5¸ Al/Si=100/HZSM-5) [8], clay mineral (Kaolin) and oxides (CaO, ZnO) [9], metal-loaded modified H-ZSM-5 (Mg/ZSM-5, Zn/ZSM-5, Ni/ZSM-5, H/ZSM-5, Cu/ZSM-5, Ga/ZSM-5, Co/ZSM-5) [10], Co-modified HZSM-5 (HZSM-5, 3Co-H-5) [11], modified HZSM-5 (HZSM-5, P/HZSM-5, Zn/HZSM-5, Ti/HZSM-5) [12], Fe-modified ZSM-5 zeolite (ZSM-5, 0.5%Fe/ZSM-5, 1%Fe/ZSM-5, 2%Fe/ZSM-5, 4%Fe/ZSM-5, 8%Fe/ZSM-5) [13], transition metal-modified ZSM-5 zeolite (ZSM-5, CoO, Co_3O_4, Co(5%)/ZSM-5, Co(10%)/ZSM-5, NiO, Ni(1%)/ZSM-5, Ni(5%)/ZSM-5, Ni(10%)/ZSM-5) [14], metal promoted ZSM-5 (HZSM-5, Co/HZSM-5, Ni/HZSM-5) [15], HZSM-5 with hierarchical structure (HZSM-5, Hi-ZSM-5, La/Hi-ZSM-5) [16], faujasite zeolite (Na-FAU, $Na_{0.2}H_{0.8}$-FAU, H-FAU) [17], mesoporous aluminosilicates (MSU-S/H_{BEA}, MSU-S/W_{BEA}, Al-MCM-41) [18], molecular sieves (HZSM-5, ZMCM-10%, ZMCM-30%, ZMCM-50%, ZMCM-70%, ZMCM-90%, MCM-41) [19], β-zeolites (SAR 21, SAR 25, SAR 38, SAR 75, SAR 250) [21], acid ZSM-5 (SAR 23, SAR 30, SAR 80, SAR 280) [22], (TiO_2-Anatase, 5 wt%-Ni/TiO_2, 5 wt%-Pt/TiO_2, CeOx–TiO_2, CeO_2, ZrO_2, MgO) [24], Ce-loaded HZSM-5 (HZSM-5, Ce/HZSM-5) [25], Ce-modified zeolite Y (ZSM-5, Ce-ZSM 5, Zeolite Y, Ce-zeolite Y) [26], silicon carbide foam supported ZSM-5 composite [29], hierarchical Y-type zeolites (TY0, TY1, and TY2) [32], Ce-modified hierarchical ZSM-5 [34].

All the studies on catalytic upgrade of pyrolysis volatiles have been focused on deoxygenation of bio-oil [1-34], but emphasis has also been given on the conversion of BTEXN [3, 5-6, 10-11, 13, 15, 28-30, 32], as well as reaction mechanism/pathway [3-4, 6-8, 10-11, 19, 23-24, 30]. The catalytic upgrade of pyrolysis volatiles has been carried out by flash pyrolysis/analytical pyrolysis (Py–GC/MS) [1-2, 5, 15, 21-22, 24, 32], by flash pyrolysis [3-4, 6, 11, 34], as well as by vacuum pyrolysis [8, 12, 16, 19], in drop-tube reactors [3-4, 6, 11, 23, 30], fixed bed reactors [7-10, 13, 25-26, 31], and fluidized bed reactors [31]. The catalytic upgrade of pyrolysis volatiles were performed in micro [1-2, 5, 15, 21-22, 24, 32], bench [18], and laboratory [3-4, 6-7, 8-14, 16-17, 19-20, 23, 25-26, 28-31, 34]. The catalytic upgrade processes operated in batch [7-10, 12-14, 16-17, 21, 25-26, 28-29], and continuous mode [1, 3-4, 6, 11, 23, 30-31], and only a few studies operated as a two-stage reactor, that is, using a process schema consisting of a thermal cracking reactor coupled to a catalyst fixed bed reactor [8, 12-13, 16-17, 19, 26, 31].

The reaction products by the catalytic upgrade of pyrolysis bio-oils from *lignocelullosic biomass* [1, 7-8, 10, 12-14, 16-19, 21-22, 24-25, 29, 31], *lignin* [28, 30], corn Stover [29], *cellulose* [30, 34], *coal/lignite* [2-6, 11, 23, 32], *lipid-base materials* [9, 15], *monosaccharides* (glucose) [30], and *waste tires granules* [26] include gaseous and liquid fuels**,** water, aqueous acid phase, and coke [6-8, 10, 16-19, 23, 28-30, 35-47].

The investigated physicochemical properties by the catalytic upgrade of pyrolysis bio-oils includes the viscosity [8-9, 12, 16, 19], specific heat [9], high heating value [8, 10, 12, 16-17, 19], cloud point [9], density [8, 12, 16, 19], water content [8-10, 17], and pH [8-9, 12, 16-17, 19].

The pyrolysis bio-oil are composed by alkanes, alkenes, ring-containing alkanes, ring-containing alkenes, cyclo-alkanes, cyclo-alkenes, and aromatics [8-9, 15, 19, 25, 28-29, 31], and oxygenates including carboxylic acids, aldehydes,

ketones, fatty alcohols, phenols, amines, amides, ethers, and esters [8-9, 15, 19, 25, 28-29, 31].

Beyond the operating mode (batch, continuous), type of pyrolysis process (flash pyrolysis/analytical pyrolysis, flash pyrolysis, and vacuum pyrolysis), type of reactors (drop-tube reactors, fixed bed reactors, and fluidized bed reactors), as well as process schema (two-stage reactor), other process parameters/variables that may affect the yields and quality of bio-oil pyrolysis by catalytic upgrade of pyrolysis volatiles are temperature [2, 4, 6, 8-9, 11, 24, 28, 31], catalyst-to-biomass [8-9, 15, 25, 28-29], characteristics of feed material including coal [2-6, 11, 23, 32], lignocelullosic biomass [1,7-10, 12-19, 21-22, 24-26, 28-31, 34], gas flow rate [31], weight hour space velocity (WHSV) [31], and the process scale [8-9, 15, 25, 28-29].

Despite some studies focusing the effect of catalyst-to-biomass ration on the yield and chemical composition of bio-oil pyrolysis by catalytic upgrade of pyrolysis vapors in micro [15], and laboratory [8-9, 25, 28-29], *until the moment, no systematic study has investigated the effect of catalyst-to-biomass ratio on the yield, chemical composition and physicochemical properties (density, kinematic viscosity, and acidity) of bio-oil pyrolysis in semi-pilot scale, using a two-stage reactor schema, as well as the influence reaction time on hydrocarbons and oxygenates composition and physicochemical properties of bio-oil pyrolysis*. The effect of catalyst-to-biomass ratio on the yield and chemical composition of bio-oil pyrolysis by catalytic upgrade of pyrolysis vapors [8-9, 15, 19, 25, 28-29], summarized as follows.

Fan *et. al.* [8], investigated influence of process parameters (temperature, catalyst-to-biomass ratio, catalyst Si/Al ratio) on the yield and composition of liquid phase by the catalytic upgrading of vapors from the vacuum pyrolysis of rape straw over nanocrystalline HZSM-5, using fixed bed reactor in a two-stage reactor schema in laboratory scale. The fixed bed pyrolysis reactor (φ_{id} = 60 mm, H = 150 cm, $V_{Reactor}$ = 4241 mL), placed bellow the catalytic reactor, was coupled to a catalytic reactor (φ_{id} = 40 mm, H = 100 mm, $V_{Reactor}$ = 125.6 mL). The experiments were carried out at 400, 450, 500, 550 and 600°C, biomass-to-catalyst ratios of 1.0, 0.5, 1/3, 0.25, and 0.2, HZSM-5 Si/Al ratios of 25, 50, 75, and 100, using particles of rape straw within the range of 100–150 μm. For the experiments with varying temperature, biomass-to-catalyst ratio of 1/3 and HZSM-5 Si/Al ratio of 50, the yield of liquid phase varied between 33.24 and 42.65% (wt.), showing a decrease with increasing temperature. For the experiments with varying biomass-to-catalyst ratio, 500 °C and HZSM-5 Si/Al ratio of 50, the yield of liquid phase varied between 29.24 and 43.15% (wt.), showing a decrease with decreasing biomass-to-catalyst ratio. For the experiments with varying HZSM-5 Si/Al ratio, 500 °C and biomass-to-catalyst ratio, the yield of liquid phase varied between 29.24 and 43.15% (wt.), showing an increase with increasing HZSM-5 Si/Al ratio. The optimize operating conditions were 500 °C, HZSM-5 Si/Al ratio of 50, and biomass-to-catalyst ratio of 1/3. The pH, density and viscosity of bio-oil were 5.15, 0.96 (g/cm^3) and 5.12 (mm^2/s) respectively. The GC-MS analysis shows that catalytic upgrading of pyrolytic vapors from the vacuum pyrolysis of rape straw increases substantially the content of aromatics and hydrocarbons, while those of phenols decrease.

Li *et. al.* [19], investigated the effects of mixing ratios catalysts (HZSM-5, MCM-41) in different proportions using in situ catalytic in the upgrading of biomass-derived pyrolysis vapors of rape straw, enjoying fixed bed reactor in a two-stage reactor schema in laboratory scale. The fixed bed pyrolysis reactor (φ_{id} = 60 mm, H = 150 cm, $V_{Reactor}$ = 4241 mL), placed bellow the catalytic reactor, was coupled to a catalytic reactor (φ_{id} = 42 mm, H = 116 mm, $V_{Reactor}$ = 160.7 mL). The experiments were carried out at 500 °C using different mixing ratios HZSM-5, 90%HZSM-5/10%MCM-41, 70%HZSM-5/30%MCM-41, 50%HZSM-5/50%MCM-

 doi:10.20944/preprints202204.0017.v1

41, 30%HZSM-5/70%MCM-41, 10%HZSM-5/90%MCM-41, and MCM-41. The experimental results show that increasing the MCM-41 proportion causes a decrease on the yield of bio-oil from 23.0 to 17.61% (wt.) until the mixing ratio proportion of 50%, whereas an increase on the yield of bio-oil from 17.61 to approximately 26.0% (wt.) is observed for mixing ratio proportion higher than 50% (wt.). The physicochemical properties using mixing ratios 50%HZSM-5/50%MCM-41 gives the best results. That way, the pH, density and viscosity of bio-oil were 5.41, 0.94 (g/cm³) and 5.06 (mm²/s) respectively. The GC/MS analysis shows that hydrocarbon content in the bio-oil organic phase gradually increased and the carbonyl groups content gradually decreased, as the MCM-41 content increased from 0 to 50%. In contrast, the hydrocarbon content gradually decreased and the carbonyl groups content gradually increased, as the MCM-41 content increased from 50% to 100%. The GC/MS analysis identified aromatic hydrocarbons, as well as oxygenates including phenols, ketones, aldehydes, carboxylic acids, and alkohols.

Koul *et. al.* [9], investigated the effect of catalyst-to-biomass ratio on the yield of bio-oil organic phase by the catalytic upgrading of vapors from castor seed oil pyrolysis over different catalysts (Kaolin, CaO, ZnO), using fixed bed reactor in a two-stage reactor schema in laboratory scale. In addition, for the experiments giving the highest yields, the physicochemical properties including pH and kinematic viscosity were determined. The fixed bed pyrolysis reactor (φ_{id} = 6 cm, H = 21 cm, $V_{Reactor}$ = 593.7 mL), containing the castor seed oil (40 g), is separated 2.0 cm from the catalyst bed using glass wool in between. The experiments were carried out at 550 °C, heating rate of 25 °C/min, using 5, 10, 15, and 20 % (wt.) catalyst. The results show that the highest bio-oil yields were obtained using 15% (wt.) Kaolin, 15% (wt.) CaO, and 10% (wt.) ZnO. The highest bio-oil yields were 64.9, 66.4, and 65.8% (wt.) using Kaolin, CaO and ZnO, respectively, showing pH values of 8.36, 9.25 and 8.32, while the measured kinematic viscosity were 39.0, 8.3 and 28.0 (mm²/s). The FT-IR analysis identified the presence of hydrocarbons (alkanes, alkenes, and alkynes), as well as oxygenates (acids, aldehydes, ketones, esters, and amines). The GC-MS analysis of bio-oils obtained by catalytic upgrading of castor seed pyrolytic vapors using 15% (wt.) Kaolin, 15% (wt.) CaO, and 10% (wt.) ZnO identified the presence of aromatics, esters, amines, acids, alkanes, amides, alkenes, alcohols, ethers, as well as non-identified compounds, showing hydrocarbons contents (aromatics, alkanes, alkenes) of 21.92 (area.%), 12.43 (area.%), and 37.49 (area.%), respectively.

Vichaphund *et. al.* [15], investigated the influence of catalyst-to-biomass ratio on the yield and chemical composition of bio-oil organic phase by the catalytic upgrading of Jatropha waste pyrolysis vapors over Co and Ni impregnated HZSM-5, nanocrystalline HZSM-5, using flash pyrolysis/analytical pyrolysis (Py-CG/MS). The experiments were carried out at 500 °C, 30 seconds, using HZSM-5, Co/HZSM-5, and Ni/HZSM-5, and catalyst-to-biomass ratios of 1.0, 5.0, and 10.0. The experiments show for all the catalysts the yield of bio-oil organic phase decreases with increasing catalyst-to-biomass ratios. The GC-MS analysis show that hydrocarbons content (aliphatic, aromatics) increases drastically with increasing catalyst-to-biomass ratios, varying between 30.43 and 96.3% (area.%) for HZSM-5, between 31.96 and 95.33% (area.%) for Co/HZSM-5, and between 34.76 and 97.55% (area.%) for Ni/HZSM-5. The highest yield of bio-oil organic phase was obtained with Ni/HZSM-5, catalyst-to-biomass ratio of 1:1, being approximately to 53.0% (wt.). The Py-GC-MS analysis identified hydrocarbons (aliphatic and aromatic) and oxygenates (esters, ethers, sugars, phenols, ketones, alcohols, and carboxylic acids).

Balasundram *et. al.* [25], investigated the effect of catalyst-to-biomass ratio on the yield and hydrocarbons composition of bio-oil by the catalytic upgrading

 doi:10.20944/preprints202204.0017.v1

of sugarcane bagasse pyrolysis vapors over Cerium (Ce) loaded HZSM-5, using a tubular furnace reactor in laboratory scale. The experiments were carried out at 500°C, catalyst-to-biomass ratios of 0.5, 1.0, 1.5, and 2.0 of HZSM-5 and Ce/HZSM-5, using dried, ground and sieved sugarcane bagasse particle of less than 0.5 mm. The results show that the yield of pyrolysis oil is higher using (Ce) loaded HZSM-5. In addition, the yields of pyrolysis oil varied between 58.0 and 68.0% (wt.). For the experiments using (Ce) loaded HZSM-5, the yield of pyrolysis oil increase with increasing catalyst-to-biomass ratio between 58.0 and 68.0% (wt.). The hydrocarbons content in pyrolysis bio-oil is higher using HZSM-5 compared to (Ce) loaded HZSM-5. In addition, for the experiments using HZSM-5, the hydrocarbons content in pyrolysis bio-oil increases with increasing HZSM-5-to-biomass ratio. The GC-MS analysis identified hydrocarbons and oxygenates (esters, ethers, anhydrosugars, phenols, furans, ketones, alcohols, and carboxylic acids).

Fan *et. al.* [28], investigated influence of process temperature and catalyst-to-biomass ratio on the yield and chemical composition of pyrolysis oil by the catalytic upgrading of vapors from microwave-assisted vacuum pyrolysis of lignin over HZSM-5, in laboratory scale. The experiments were carried out at 450 °C, catalyst-to-lignin ratios of 0, 0.1, 0.2, 0.3, 0.4, and 250, 350, and 550 °C, catalyst-to-lignin ratios of 0.3. For the experiments with varying catalyst-to-lignin ratios, the yield of pyrolysis bio-oil varied between 34.11 and 21.75% (wt.), showing a decrease with increasing catalyst-to-lignin ratios. In addition, the content of polycyclic aromatic hydrocarbons and monocyclic aromatic hydrocarbons increases with increasing catalyst-to-lignin ratios. For the experiments with varying temperature, the yield of pyrolysis bio-oil varied between 28.11 and 23.30% (wt.), showing no variation between 250 and 350 °C and a decrease between 350 and 550 °C. In addition, the content of polycyclic aromatic hydrocarbons increases with increasing temperature, while the content monocyclic aromatic hydrocarbons increases between 250 and 450 °C, decreasing between 450 and 550 °C. The GC-MS analysis identified polycyclic aromatic hydrocarbons (PAHs), monocyclic aromatic hydrocarbons (MAHs), as well as oxygenates (phenols, carboxylic acids, aldehydes, and ketones).

Zhou *et. al.* [29], investigated influence of 02 (two) different ex-situ configurations with randomly packed bed and composite catalysts bed, as well as the effect of catalyst-to-biomass ration for ex-situ composite catalysts bed on the yield and chemical composition of pyrolysis oil, expressed in peak area, by the catalytic upgrading of vapors from microwave-assisted vacuum pyrolysis of corn Stover over Silicon carbide foam supported ZSM-5, in laboratory scale. The experiments were carried out by setting the pyrolysis reactor temperature and catalyst bed temperature at 550 °C and 425 °C, respectively. For the ex-situ configurations experiments with randomly packed bed and composite catalysts bed, pyrolysis reactor temperature and catalyst bed temperature at 550 °C and 425 °C, and catalyst-to-biomass ratio of 0.25, the yield of pyrolysis bio-oil is higher for the ex-situ configurations with composite catalysts bed. In addition, the ex-situ composite catalyst bed configuration produced a pyrolysis bio-oil of higher quality, showing 41.5% (area.) aromatics and only 1.6% (area.) oxygen-containing aliphatic, while the ex-situ with randomly packed bed produced pyrolysis bio-oil containing 27.8% (area.) aromatics and 11.7% (area.) oxygen-containing aliphatic. For the ex-situ configurations experiments with composite catalysts bed, pyrolysis reactor temperature and catalyst bed temperature at 550 °C and 425 °C, and catalyst-to-biomass ratio of 0, 0.1, 0.25, and 0.5, the yield of pyrolysis bio-oil varied between 41.0 to 33.0% (wt.), decreasing with increasing catalyst-to-biomass ratio. In addition, the content of aromatic hydrocarbons and BTEX in pyrolysis bio-oil increases with increasing catalyst-to-biomass ratio. The

 doi:10.20944/preprints202204.0017.v1

Py-GC-MS analysis identified aliphatic hydrocarbons, aromatic hydrocarbons, polycyclic aromatic hydrocarbons (PAHs), BTEX, and oxygenates (furans, carboxylic acids, and phenols).

The objective of this work was to investigate the effect of catalyst-to-biomass ratio (0.05, 0.075, 0.100) and reaction time (40, 50, 60, 70, and 80 minutes) by the catalytic upgrading of pyrolysis vapors of residual fat at 450 °C and 1.0 atmosphere, on the yield, physicochemical properties (density, kinematic viscosity, refractive index, and acid value) and chemical composition of hydrocarbons (alkanes, alkenes, and aromatics) and oxygenates (carboxylic acids, esters, ketones, aldehydes, of pyrolysis bio-oils, over a catalyst fixed bed reactor containing 0.0, 5.0, 7.5, and 10.0% (wt.) Red Mud pellets activated with 1.0 M HCl, in semi-pilot scale, using a process schema consisting of a two-stage reactor, whereas the first stage is a pyrolysis reactor of 2.0 L coupled to the second-stage, a catalyst fixed bed reactor of 53 mL, in batch mode.

2. Materials and Methods

2.1. Methodology

The process flow sheet shown in Figure 1 summarizes the applied methodology, described in a logical sequence of ideas, chemical methods, and procedures to produce liquid hydrocarbon mixtures by catalytic upgrading of residual fat pyrolysis vapors/volatiles at 450 °C and 1.0 atm, over a catalyst fixed bed reactor, using a activated Red Mud pellets catalyst, in semi pilot scale. Initially, the residual fat is collected. Afterwards, it is subjected to pre-treatment (sieving) and separation processes (evaporation, dehydration). The Red Mud is dried, milled, and sieved to reduce the particle size. Afterwards, activated with HCl and the pellets formed by pressing and drying followed by thermal activation. The experiments were carried out using a process schema consisting of a pyrolysis reactor coupled to a catalyst fixed bed reactor, with and without catalyst. The effect of catalyst content and reaction time was analyzed. The physical-chemistry properties and chemical composition of hydrocarbon rich liquid mixtures determined.

 doi:10.20944/preprints202204.0017.v1

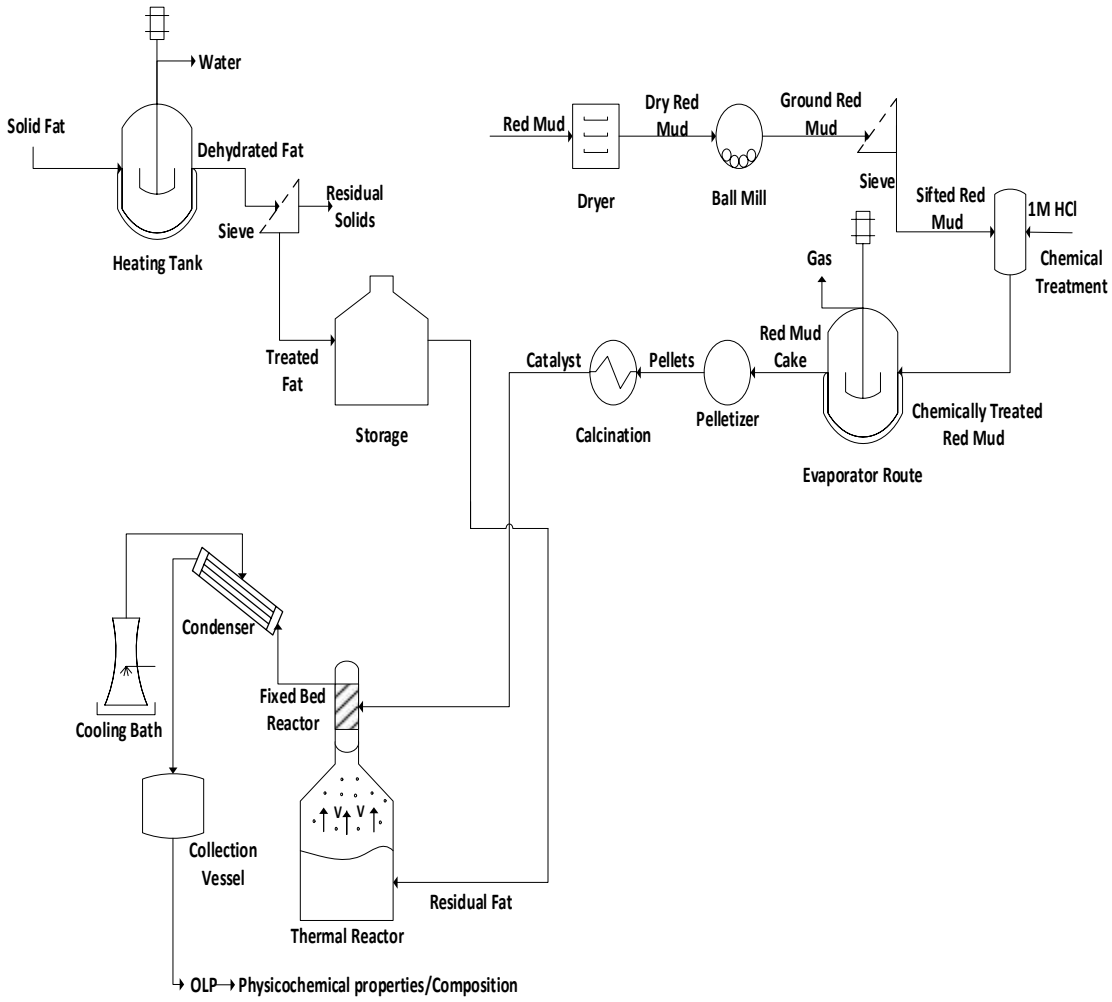

Figure 1. Process flowsheet by the production of hydrocarbon liquid mixtures by thermal cracking and thermal catalytic cracking of residual fat at 450 °C, 1.0 atm, 5.0, 7.5, and 10.0% (wt.) of Red Mud pellets activated with 1.0 M HCl, using a catalyst fixed bed reactor, in semi pilot scale.

2.2. Materials

The residual fat was collected from a system of fat-retaining boxes at University Restaurant of UFPA. The residual fat was submitted to pre-processing (heating, homogenization) and separation processes (dehydration, sieving), as described elsewhere [35]. By the pre-processing, the fat was subjected to heating and mechanical agitation in order to evaporate the excess moisture and homogenize the lipid-base mixture. Afterwards, the liquified fat material was sieved to remove suspended and undesired solid materials, as described synthetically in flowsheet of Figure 1. The residual fat after pre-processing is illustrated in Figure 2.

Figure 2. Pre-treated residual fat used as feed material by thermal catalytic cracking at 450 °C, 1.0 atm, 0.0, 5.0, 7.5, and 10.0% (wt.) Red Mud pellets activated with 1.0 M HCl, using a catalyst fixed bed reactor, in semi pilot scale.

2.3. Production of red mud activated pellets

Pellets of Red Mud, chemically activated with 1.0 M HCl, were used as catalysts, and the procedures described in details in flowsheet illustrated in Figure 1.

2.3.1. **Physical pre-treatment of red mud**

The physical pre-treatment of Red Mud takes place in several steps, as illustrated in Figure 1. In this sense, a more detailed description of each pre-treatment step (drying, milling, and sieving) should be highlighted for a better understanding as follows. First, the Red Mud was subjected to drying using an oven (Model Bio SEA - 40L) for a period of 08 (eight) hours, at a temperature of 105 °C, to remove the excess water present. 1000 grams of Red Mud was used each batch. The material was weighed every hour to compute the drying curve. Afterwards, the dried Red Mud was grinded using a ball mill (Brand: CIMAQS, Series Nº. 005) in order to reduce the particle size. 5.5 kg of dried Red Mud was processed by each grinding/milling for 01 (one) hour. Then, the dried and grinded Red Mud were submitted to sieving process to select only particles with particle size smaller than 65 MESH sieve (0.210 mm). A total of 25 sieving batches were carried out. Red Mud before and after the pre-treating of drying, milling and sieving is shown in Figure 3.

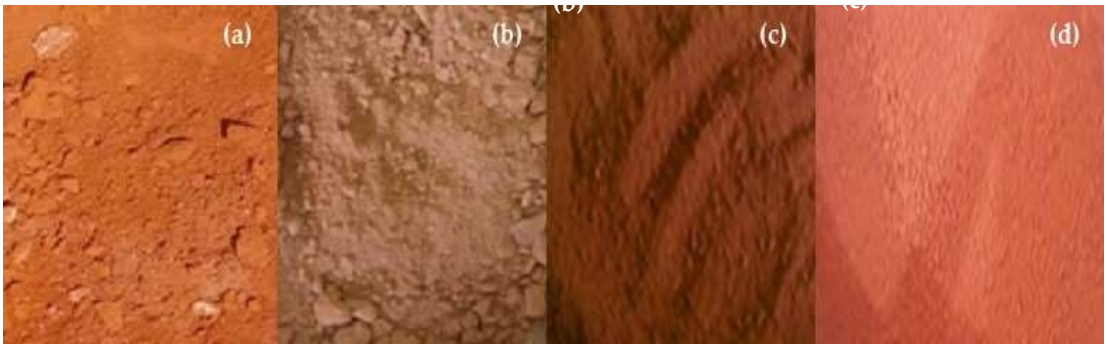

Figure 3. Material after drying, milling and sieving process of Red Mud [Red Mud (a); Dried Red Mud (b); Comminuted Red Mud (c); Sieved Red Mud (d)].

2.3.2. **Chemical activation of red mud**

After the physical pre-treatment described in section 2.3.1, the Red Mud was activated chemically with HCl and the procedures described as follows: 1-

 doi:10.20944/preprints202204.0017.v1

100 g of dried, grinded, and sieved Red Mud was mixed with 150 g of a 1.0 M HCl solution using a Becker of 1000 mL. The addition of 1.0 M HCl solution into the fine Red Mud powder produced a moisture cake, making it necessary to remove the excess moisture by using a heating plate at 100 °C with analogic temperature control [] for 80 minutes. By removing the excess moisture, the cake changes its physical consistency to a pasty cake suitable for shaping. Red Mud fine powders mixed with 1.0 M HCl solution (a) and Red Mud pasty cake (b) is shown in Figure 4.

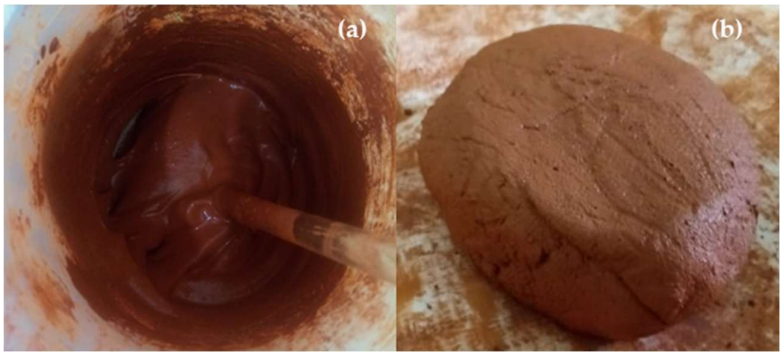

Figure 4. Processing of pre-treated Red Mud fine powders with 1.0 M HCl solution [Red Mud fine powders mixed with 1.0 M HCl solution (a); Red Mud pasty cake (b)].

2.3.3. **Production of pellets**

For the production of pellets, an acrylic mold with cylindrical holes of approximately 0.70 cm was constructed used, as shown in Figure 5. The activated Red Mud pasty cake was placed manually in the mold openings, giving the material the desired shape. After molding, the pellets were submitted to calcination using a muffle (NETLAB, Model SSFM6L) at 500 °C for a period of 04 hours. The calcination process aims to improve the textural properties, particularly the catalyst specific area, as well as the pellets thermal stability. The acrylic mold and the pellets before and after calcination is shown in Figure 5.

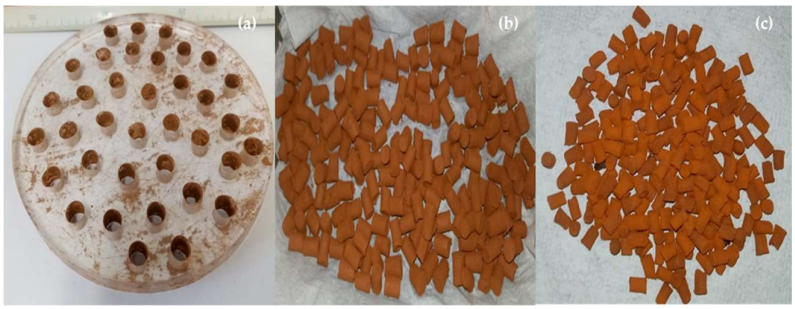

Figure 5. Production of activated Red Mud Material pellets before and after calcination [Acrylic mold (a); Red Mud pellets before calcination (b); Red Mud pellets after calcination (c)].

2.4. Characterization of residual fat

The pre-treated residual fat was physicochemical characterized for density, refractive index and acid value according to official methods AOCS Cc 10c-95, AOCS Cc 7-25, and AOCS Cd3d-63 [35-37]. In a previous study, kinematic viscosity of residual fat was determined according to ASTM D 2515 method [35-39].

2.5. Experimental apparatus and procedures

2.5.1. **Experimental apparatus**

Preprints (www.preprints.org) | NOT PEER-REVIEWED | Posted: 4 April 2022 doi:10.20944/preprints202204.0017.v1

The thermal catalytic cracking unit with a fixed bed reactor in semi pilot, depicted in Figure 4, described in details elsewhere [36]. By the thermal catalytic cracking experiments, at the output of pyrolysis/batch reactor (R-1), a second AISI 304 stainless steel fixed bed reactor (R-2) is coupled. The fixed bed reactor (R-2) of cylindrical geometry has 30 cm height and 15 mm internal diameter ($V_{(R-2)}$ = 53 ml). An spiral-shaped electrical resistance, with 1.5 kW, was inserted around the reactor (R-2). A glass wool thermal blanket was used as a thermal insulator in order to avoid energy loss to the environment. A type K, sheath thermocouple (550 °C) is placed inside the reactor (R-2) for measuring its temperature. Figure 5 shows the schematic diagram of bench scale catalytic cracking unit with a fixed bed (R-2).

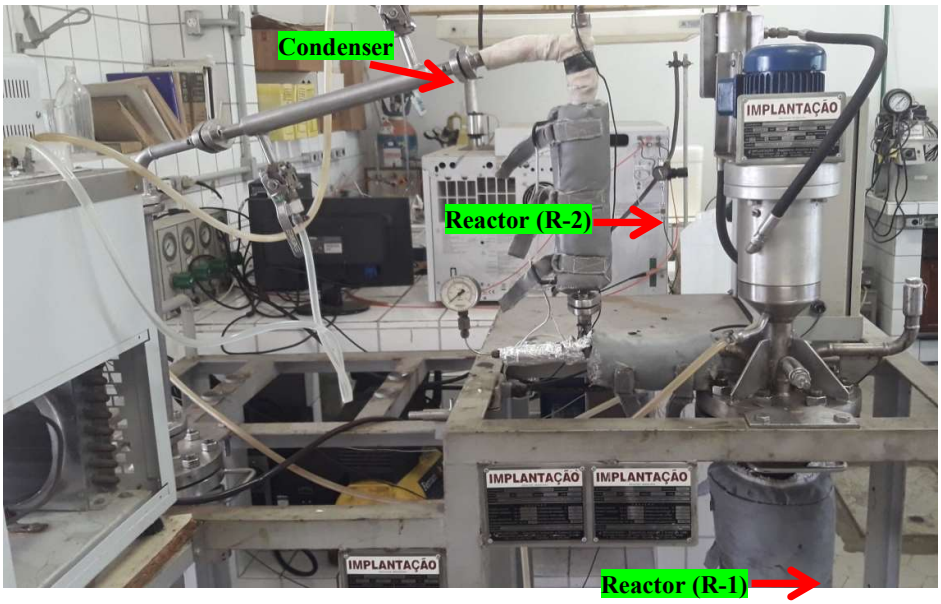

Figure 4. Thermal catalytic cracking unit with a pyrolysis reactor (R-1) and a fixed bed reactor (R-2) in bench scale.

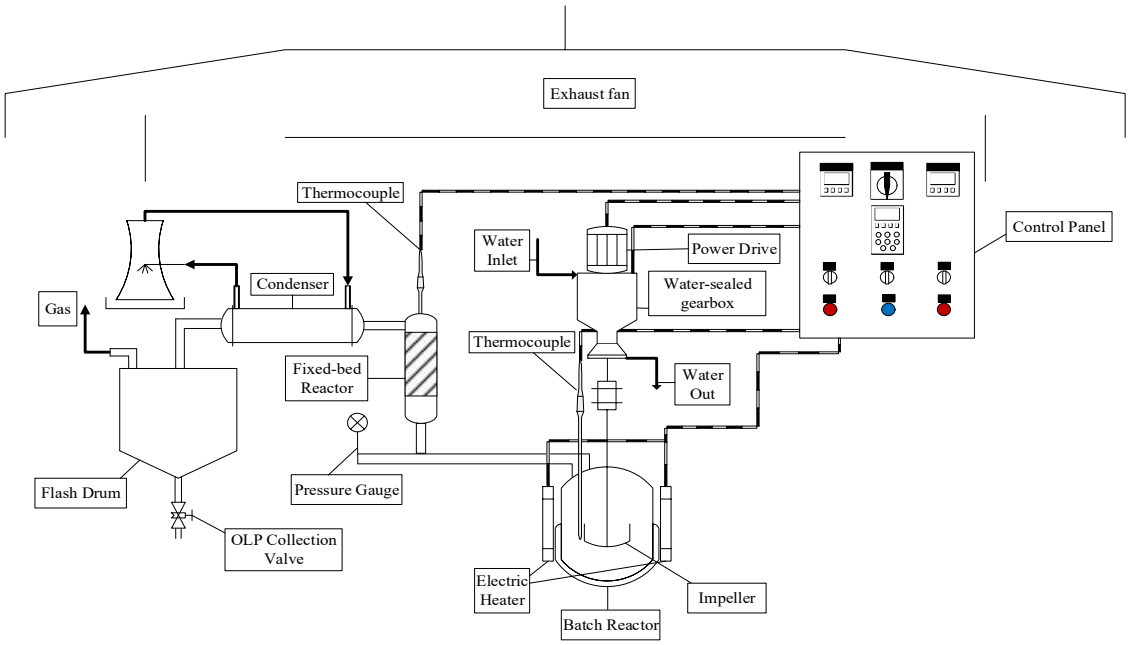

Figure 5. Schematic diagram of bench scale stainless steel catalytic cracking reactor with a pyrolysis/batch reactor and a fixed bed reactor.

 doi:10.20944/preprints202204.0017.v1

2.5.2. Experimental procedures

2.5.2.1 Pyrolysis

By the thermal cracking (pyrolysis) of residual fat, the residual fat was weighed (1000 g) using an electronic balance (Mars, AL500). Afterwards, the residual fat is added within the stirred tank reactor (R-1), whereas pyrolysis takes place. After sealing the reactor, the experimental apparatus has been set up. Then, the cooling system is turned on and the water temperature was set at 10 °C. Afterwards, the programming step is carried out, thus making it possible to set the desired operating parameters, including heating rate (10 °C/min), cracking temperature (450 °C) and the mechanical impeller speed (100 rpm). After the experiment starts, the operational parameters (heating rate, cracking temperature, and mechanical impeller speed) were recorded every 10 minutes. By each thermal cracking experiment, 04 (four) samples were withdrawn along with the reaction time in order to study and/or investigate the reaction kinetics of organic liquid products. In addition, the non-condensable gases were burned at the exit of the gas pipeline line (gas flare). The mass of solid phase products (coke) was collected and weighed, and the mass of gas computed by difference. The yield of reaction products computed by applying a mass balance, closed thermodynamic system, batch mode, stationary process. The organic liquid products (OLP) were submitted to pre-treatments of decantation to remove water and filtration. Then, organic liquid products (OLP) physicochemical characterized by density, kinematic viscosity, refractive index, and acid value.

2.5.2.2 Thermal catalytic cracking

By the thermal catalytic cracking experiments, the activated Red Mud pellets were first introduced inside the fixed bed reactor (R-2). Afterwards, the reactor (R-2) was vertically coupled between the reactor (R-1) and the condenser, as shown in Figure 4. Then, the desired operating parameters are set up, including the heating rate (10 °C/min), cracking temperatures (450 °C) of both reactors (R-1) and (R-2), as well as the mechanical impeller speed (100 rpm). Furthermore, the temperature of fixed bed reactor (R-2) was set up approximately 10 °C/20 °C higher than that of reactor (R-1) in order to avoid condensation of ascending vapors produced inside the reactor (R-1) through the porous of pellets catalyst and between the void volume of fixed bed reactor (R-2). That is, thermal cracking of residual fat takes place in reactor (R-1), producing an ascending vapor phase (gas phase reaction products) that flows through the porous of pellets catalyst and between the void volume of fixed bed reactor, whereas a heterogeneous gas-solid reaction takes place in catalyst fixed bed (R-2). The thermal catalytic cracking experiments carried out with 5.0, 7.7, and 10.0% (wt.) chemically activated Red Mud pellets inside the fixed bed reactor (R-2). By each thermal catalytic cracking experiment, 04 (four) samples were withdrawn along with the reaction time in order to study and/or investigate the reaction kinetics of organic liquid products. In addition, the non-condensable gases were burned at the exit of the gas pipeline line (gas flare). The mass of solid phase products (coke) was collected and weighed, and the mass of gas computed by difference. The yield of reaction products computed by applying a mass balance, closed thermodynamic system, batch mode, stationary process. The organic liquid products (OLP) were submitted to pre-treatments of decantation to remove water and filtration. Then, organic liquid products (OLP) physicochemical characterized by density, kinematic viscosity, refractive index, and acid value.

2.6. Physical-chemistry analysis and chemical composition of OLP

2.6.1. Physical-chemistry analysis of OLP

Preprints (www.preprints.org) | NOT PEER-REVIEWED | Posted: 4 April 2022 doi:10.20944/preprints202204.0017.v1

The organic liquid phase products (OLP) were physicochemical analyzed for acid value, density at 25 °C, kinematic viscosity at 40 °C, and refractive index according to official methods, as described elsewhere [35-39].

2.6.2. Chemical composition of organic liquid products

The chemical composition of OLPs were determined by CG-MS and the equipment and procedures described in details by Castro *et. al.* [38]. The peak intensity, retention times, and compounds identification were analyzed according to the NIST mass spectra library. The concentrations were expressed in area, as no internal standard was injected to compare the peak areas.

2.7. Characterization of activated red mud pellets

2.7.1. SEM and EDX analysis

The morphological characterization of chemically activated red mud pellets performed by scanning electron microscopy using a microscope (Tescan GmbH, Czech Republic, Model: Vega 3). The samples were covered with a thin layer of gold using a Sputter Coater (Leica Biosystems, Germany, Model: Balzers SCD 050). Elemental analysis and mapping were carried out by energy dispersive x-ray spectroscopy (Oxford instruments, UK, Model: Aztec 4.3).

2.7.2. XRD analysis

The crystalline characterization of chemically activated red mud pellets performed by x-ray diffraction using a diffractometer (Rigaku, Japan, Model: MiniFlex600) at the Laboratory of Structural Characterization (FE-MAT/UNIFESSPA) and the equipment specifications described as follows: *generator* (maximum power: 600 W; tube voltage: 40 kV; tube current: 15 mA; X-ray tube: Cu), *optics* (fixed divergence, scattering and receiving slit; filter; Kβ sheet; monochromator: graphite; soller slit: 5.0°), *goniometer* (model: vertical, radius: 150 mm, scanning range: -3 A , 145° (2θ); scanning speed: 0.01 to 100°/min (2θ); accuracy: ± 0.02°) and *detector* (high-speed silicone tape).

2.8. Mass balances by catalytic cracking of vapor phase products

Application of mass conservation principle in the form an overall mass balance within the pyrolysis reactor, operating in batch mode, open thermodynamic system, yields the following equations for the material system R-1 (pyrolysis reactor).

$$\dot{m}_{in,pyrolysis} - \dot{m}_{out,pyrolysis} = \frac{dm_{Feed}}{d\tau} \quad (1)$$

$$\dot{m}_{in,pyrolysius} = 0 \quad (2)$$

$$-\dot{m}_{out,pyrolysis} = \frac{dm_{Feed}}{d\tau} \quad (3)$$

$$-\dot{m}_{out,pyrolysis} = \dot{m}_{vapors,pyrolysis} \quad (4)$$

Where $\dot{m}_{in}$ is the mass flow rate entering reactor R-1, $\dot{m}_{out,pyrolysis}$ is the mass flow rate leaving the reactor R-1, $\frac{dm_{Feed}}{d\tau}$ is the time rate variation of feed mass inside reactor R-1, $\dot{m}_{vapors,pyrolysis}$ is the mass flow rate of pyrolysis vapors/volatiles leaving the reactor R-1 and entering the reactor R-2 (catalyst bed reactor). By applying an overall steady state mass balance within the catalyst reactor, operating in continuous mode, open thermodynamic system, yields the following equations for the material system R-2 (catalyst reactor). Assuming that all the vapors leaving reactor R-1, reacts at the solid pellets surface producing gaseous species, the following equations for the material system R-2 (catalyst reactor) applies.

$$\dot{m}_{vapors,pyrolysis} - \dot{m}_{out,catalyst} = \frac{dm_{vapors}}{d\tau} \quad (5)$$

$$\frac{dm_{vapors}}{d\tau} = 0 \quad (6)$$

$$\dot{m}_{vapors,pyrolysis} - \dot{m}_{out,catalyst} = 0 \quad (7)$$

 doi:10.20944/preprints202204.0017.v1

$$\dot{m}_{out,catalyst} = \dot{m}_{gas} + \dot{m}_{bio-oil} \quad (8)$$

Where $\dot{m}_{vapo\ ,pyrolysis,}$ is the mass flow rate entering reactor R-2, $\dot{m}_{out,catalyst}$ is the mass flow rate leaving the reactor R-2, $\dot{m}_{gas}$ is the mass flow rate of non-condensable gases leaving the reactor R-2, computed by difference, and $\dot{m}_{bio-oil}$ is the mass flow rate of bio-oil leaving the condenser. The mass of solid remaining in the reactor R-1 is $\dot{m}_{solid}$. By performing a steady state global mass balance within the control volume consisting of reactors R-1 and R-2 yields equation (9).

$$\dot{m}_{Feed} = \dot{m}_{solid} + m_{gas} + \dot{m}_{bio-oil} \quad (9)$$

The process performance evaluated by computing the yields of bio-oil, solid (coke), and gas defined by equations (10) and (11), and the yield of gas by difference, using equation (12).

$$Y_{bio-oil}[\%] = \frac{M_{Bio-oil}}{M_{Feed}} x100 \quad (10)$$

$$Y_{solids}[\%] = \frac{M_{Solids}}{M_{Feed}} x100 \quad (11)$$

$$Y_{gas}[\%] = 100 - (Y_{bio-o} + Y_{solids}) \quad (12)$$

4. Results

4.1. Characterization of catalyst

4.1.1 SEM analysis

The microscopies of Red Mud pellets activated with 1.0 M HCl after calcination and after upgrading of residual fat pyrolysis vapors at 450 °C, 1.0 atm, 70 minutes, with 5.0% (wt.) Red Mud pellets activated with 1.0 M HCl, in batch mode, using a semi-pilot scale reactor of 2.0 L, are illustrated in Figures 6 and 7, respectively. The microscopies of Red Mud pellets activated with 1.0 M HCl are characterized by the presence of fine round particles with sizes between 0.5 and 2.0 μm as shown in Figure 6 (c), as well as agglomerates in form of flakes with sizes between 50.0 and 300.0 μm, as described in Figure 6 (a). The SEM images are according to the results described in the literature [35, 49-52]. As previously described in the literature by Almeida *et. al.* [35], scanning electron microscopies of thermal activated Red Mud (1000 °C) show the presence of particles of irregular shape with sizes between 3.0 and 4.0 μm, as well as agglomerates of particles in form of flakes with sizes between 10 and 20 μm [35]. Mercury *et al.* [49] reported the presence of fine particles of round shape and agglomerates of particles with sizes lower than 10 μm in dried Red Mud. Li *et al.* [50] reported that activation of Red Mud with a HCl solution of 0.25 M caused surface erosion, as new cavities appeared after chemical activation with 0.25 M HCl. In addition, CaO, $CaCO_3$ and Fe_2O_3, acid-soluble oxides/salts were dissolved [50]. This is easy to observe if one compare the composition of oxides identified by XDR in Red Mud [35], with the punctual elemental analysis of activated Red Mud pellets described in Table 1. Sahu *et. al.* [51], reported the presence of rounded shape aggregates due to the presence of $Na_8(Al_6Si_6O_{24})Cl_2$ (sodalite) and $CaCO_3$ (calcite). Both sodalite and calcite are soluble in acid solutions. In addition, microscopies of activated Red Mud pellets activated with 18 g HCl 31% (wt.), dissolved in 190 g H_2O are characterized by the presence of fine round particles with sizes between 0.5 and 2.5 μm [51]. Huang *et. al.* [52], reported the SEM images of raw Red Mud are smooth and flat, while those treated with 2.0 M HCl show the appearance of cavities and coarsened exterior due to removal of some acid-soluble oxides/salts (CaO, $CaCO_3$, Fe_2O_3).

 doi:10.20944/preprints202204.0017.v1

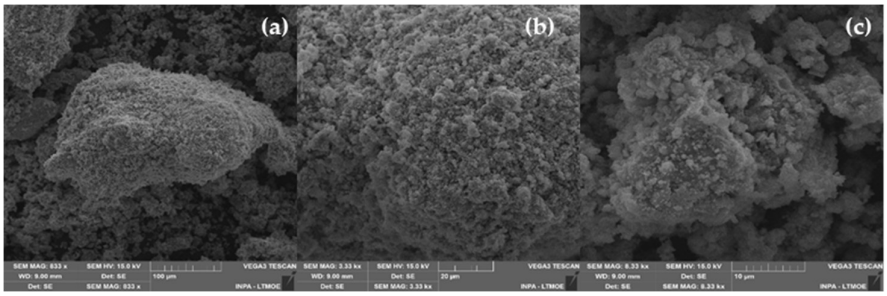

Figure 6. SEM of Red Mud pellets after calcination [MAG: 833 x (a); MAG: 3.33 kx (b); MAG: 8.33 kx (c)].

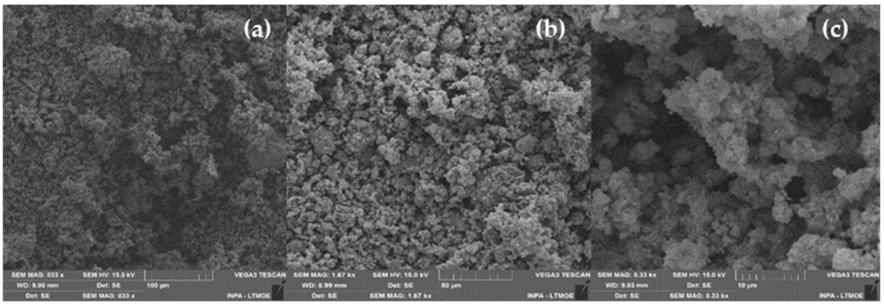

Figure 7. SEM of Red Mud pellets after upgrade of residual fat pyrolysis vapors at 450 °C, 1.0 atm, 70 minutes, with 5.0% (wt.) Red Mud pellets activated with 1.0 M HCl, in batch mode, using a semi-pilot scale reactor of 2.0 L [MAG: 833 x (a); MAG: 3.33 kx (b); MAG: 8.33 kx (c)].

SEM images of Red Mud pellets after upgrade of residual fat pyrolysis vapors at 450 °C, 1.0 atm, 70 minutes, with 5.0% (wt.) Red Mud pellets activated with 1.0 M HCl show no visual morphological difference compared to those of Red Mud pellets activated with 1.0 M HCl after calcination. In fact, the Red Mud pellets after upgrade of residual fat pyrolysis vapors became black due to the carbonization that takes place inside the pores within the solid surface.

4.1.2. EDX analysis

Table 1 shows the results of elemental analysis performed by energy dispersive x-ray spectroscopy at a point for raw Red Mud [54], Red Mud activated at 1000 °C [35], Red Mud pellets activated with 1.0 M HCl after calcination at 500 °C and 04 hours, and Red Mud pellets activated with 1.0 M HCl after upgrade of residual fat pyrolysis vapors at 450 °C, 1.0 atmosphere, using a semi-pilot scale reactor of 2.0 L. It might be observed that elemental analysis of raw Red Mud and Red Mud thermal activated at 1000 °C are similar as the same chemical elements were identified (C, O, Na, Al, Ca, Ti, Fe, and Si). By thermal activation at 1000 °C the content of sodium and aluminum decreases, while that of Fe increases, being according to results described in the literature [49]. The activation of Red Mud with a 1.0 HCl solution causes a removal of some acid-soluble oxides/salts (CaO, $CaCO_3$, Fe_2O_3), decreasing the content of carbon, calcium and iron, and increasing the content of oxygen. In addition, the chemical element chlorine has been detected, as chemical activation was caried out with HCl. After upgrading of residual fat pyrolysis vapors at 450 °C, 1.0 atmosphere, over a catalyst fixed bed reactor packed with pellets of Red Mud chemically activated with 1.0 M HCl, using a semi-pilot scale two-stage reactor of 2.0 L, one observes an increase of carbon content probably due to the adsorption of carbon molecules within the pores of catalyst surface, as gas-solid reactions takes place. In fact,

 doi:10.20944/preprints202204.0017.v1

carbonization process has been visually observed, as the color of Red Mud pellets has changed from red-iron to black.

Table 1. Percentages in mass and atomic mass of raw Red Mud, Red Mud activated at 1000 °C, Red Mud pellets activated with 2.0 M HCl after calcination at 500 °C and 04 hours, and Red Mud pellets activated with 2.0 M HCl after upgrading of residual fat pyrolysis vapors at 450 °C, 1.0 atmosphere, using a semi-pilot scale two-stage reactor of 2.0 L.

	Catalyst											
	Red Mud [54]			Red Mud 1000 °C [35]			Red Mud Pellets 2.0 M HCl			Red Mud Pellets after 450 °C		
Chemical Elements	Mass [wt.%]	Atomic Mass [wt.%]	SD	Mass [wt.%]	Atomic Mass [wt.%]	SD	Mass [wt.%]	Atomic Mass [wt.%]	SD	Mass [wt.%]	Atomic Mass [wt.%]	SD
C	15.42	24.49	0.76	13.17	23.62	0.79	-	-	-	26.20	38.31	-
O	44.79	53.30	0.63	43.77	55.97	0.72	56.11	71.95	-	40.18	44.10	-
Na	7.24	5.99	0.20	4.03	3.59	0.22	7.55	6.74	-	3.42	2.62	-
Al	7.97	5.63	1.70	3.95	2.99	0.15	12.54	9.54	-	12.54	8.16	-
Ca	1.09	0.52	0.07	1.15	0.59	0.09	0.65	0.33	-	0.55	0.24	-
Ti	1.67	0.66	0.90	1.39	0.59	0.11	1.47	0.74	-	1.14	0.42	-
Fe	15.87	5.40	0.29	29.07	10.65	0.49	12.64	4.64	-	11.99	3.77	-
Si	5.97	4.05	0.14	2.75	2.00	0.12	7.01	5.12	-	3.23	2.02	-
Cl	-	-	-	-	-	-	1.47	0.85	-	0.74	0.37	-
K	-	-	-	-	-	-	0.05	0.03	-	-	-	-
V	-	-	-	-	-	-	0.06	0.02	-	-	-	-
Ba	-	-	-	-	-	-	0.17	0.02	-	-	-	-

SD= Standard Deviation

4.1.3. XRD analysis

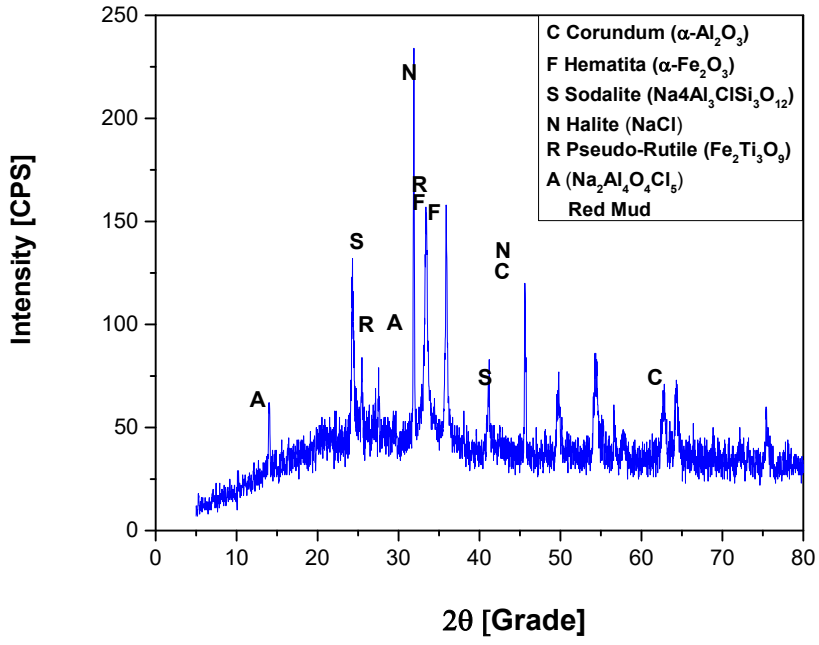

Figure 9. XRD of Red Mud pellets activated with 1.0 M HCl after calcination at 400 °C.

 doi:10.20944/preprints202204.0017.v1

Figure 9 illustrates the diffractogram of Red Mud pellets activated with 1.0 M HCl after calcination at 400 °C. The XRD shows the presence of two peaks of high intensity, the first observed on the position 2θ: 66.7 (100%), and the on the position 2θ: 45.7 (80%), both associated to the crystalline phase corundum (Al_2O_3). The peaks of high intensity associated to the crystalline phase Hematite (Fe_2O_3) were observed on the position 2θ: 33.4 (100%) and on the position 2θ: 35.8 (72.1%), being according to the results reported in the literature by Sahu *et. al.* [51], and Huang *et. al.* [52]. In addition, high intensity peaks were observed on the position 2θ: 24.5 (100%) and medium intensity on the position 2θ: 43.4 (33%), associated to the crystalline phase Sodalite ($Na_4Al_3ClSi_3O_{12}$). The crystalline phase called pseudo-rutile ($Fe_2Ti_3O_9$) was observed in two peaks of high intensity on the position 2θ: 25.4 (100%) and on the position 2θ: 33.6 (90%). The peaks of high intensity associated to the crystalline phase ($NaAl_4O_4Cl_5$) were observed on the position 2θ: 10.1 (100%) and on the position 2θ: 30.8 (80%). In addition, two peaks of high intensity peaks, associated to the crystalline phase Halite (NaCl) were observed on the position 2θ: 31.8 (100%) and on the position 2θ: 45.6 (55 %).

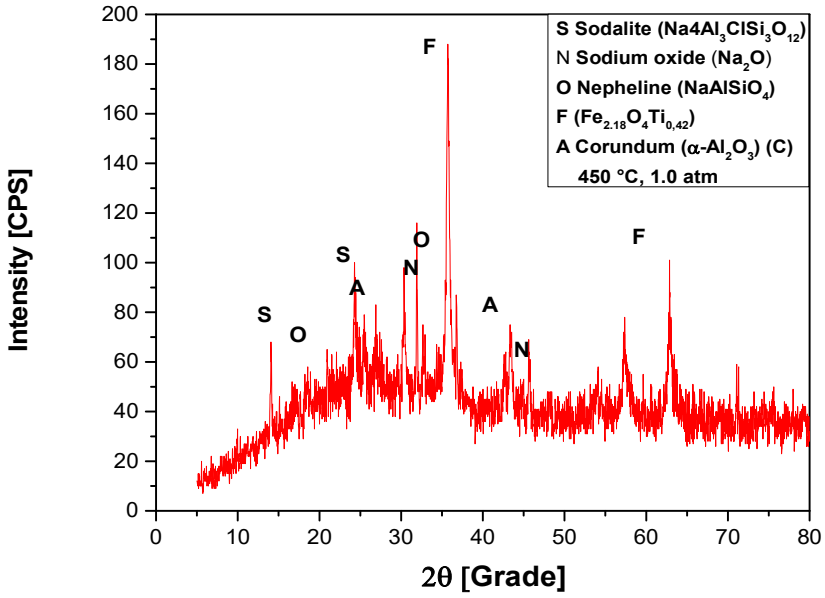

Figure 10. XRD of Red Mud pellets activated with 1.0 M HCl after the upgrading of residual fat pyrolysis vapors at 450 °C, 1.0 atmosphere, 5.0% (wt.) Red Mud pellets activated with 1.0 M HCl, using a catalyst fixed bed reactor, using a semi-pilot scale two-stage reactor of 2.0 L.

The XRD of Red Mud pellets activated with 1.0 M HCl after the upgrading of residual fat pyrolysis vapors at 450 °C, 1.0 atmosphere, 5.0% (wt.) Red Mud pellets activated with 1.0 M HCl, using a catalyst fixed bed reactor, using a semi-pilot scale two-stage reactor of 2.0 L, is shown in Figure 10. It is observed the presence of two peaks, one of high intensity, observed on the position 2θ: 24.5 (100%) and another of medium intensity on the position 2θ: 14.0 (40%), associated to the crystalline Sodalite ($Na_4Al_3ClSi_3O_{12}$). Two peaks associated to sodium oxide (Na_2O) were observed, one of high intensity on the position 2θ: 32.7 (100%) and one of low intensity on the position 2θ: 47 (37.9%). The crystalline phase Nepheline ($NaAlSiO_4$) was observed in two peaks, one of high intensity on the position 2θ: 20.8 (100%) and one of medium intensity on the position 2θ: 34.3 (56.2%). Furthermore, it was observed a peak of high intensity peaks on the

 doi:10.20944/preprints202204.0017.v1

position 2θ: 35.6 (100%) and a peak of low intensity on the position 2θ: 62.9 (35.9 %), associated to $Fe_{2.18}O_4Ti_{0.42}$. Finally, the peaks associated to the crystalline corundum phase (α-Al_2O_3) of high and low intensity were observed on the positions 2θ: 25.7 (100%) and 2θ: 43.3 (30.6%).

4.2. Upgrading of residual fat pyrolysis vapors over a catalyst fixed bed reactor

4.2.1 *Process conditions, mass balances, and yields of reaction products*

Table 2 illustrates the process parameters, mass balances, and yields of reaction products (liquids, solids, H_2O, and gas) by catalytic upgrading of residual fat pyrolysis vapors at 450 °C, 1.0 atm, 0.0, 5.0, 7.5, and 10.0% (wt.) Red Mud pellets activated with 1.0 M HCl, using a catalyst fixed bed reactor, in semi pilot scale.

Table 2. Process parameters, mass balances, and yields of reaction products (liquids, solids, H_2O, and gas) by catalytic upgrading of residual fat pyrolysis vapors at 450 °C, 1.0 atm, 0.0, 5.0, 7.5, and 10.0% (wt.) Red Mud pellets activated with 1.0 M HCl, using a catalyst fixed bed reactor, in semi pilot scale.

Process Parameters	450 (°C)			
	0.0 (wt.)	5.0 (wt.)	7.5 (wt.)	10.0 (wt.)
Mass of residual fat (g)	1000	700	700	700
Cracking time (min)	80	80	80	80
Initial cracking temperature (°C)	395	380	380	390
Mechanical system stirring speed (rpm)	90	90	90	90
Mass of solid (Coke) (kg)	66	60.05	10.92	9.1
Mass of liquid (Bio-oil) (kg)	**794.2**	**380.79**	**584.53**	**594.13**
Mass of H_2O (kg)	115	19.63	17.45	15.5
Mass of gas (kg)	24.81	239.53	104.55	81.27
Yield of Bio-oil (wt.%)	**79.42**	**54.40**	**81.76**	**84.88**
Yield of H_2O (wt.%)	11.50	2.80	2.49	2.21
Yield of Coke (wt.%)	**6.60**	**8.60**	**1.56**	**1.30**
Yield of Gas (wt.%)	**2.48**	**34.22**	**14.94**	**11.61**

The catalytic upgrading experiments of residual fat pyrolysis vapors at 450 °C, 1.0 atm, 0.0, 5.0, 7.5, and 10.0% (wt.) Red Mud pellets activated with 1.0 M HCl show bio-oil yields between 54.40 and 84.88% (wt.), aqueous phase yields between 2.21 and 11.50% (wt.), solid phase yields between 1.30 and 8.60% (wt.), and gas yields between 2.48 and 34.22% (wt.). The yields of bio-oil are according to similar studies reported in the literature for the catalytic upgrading of lipid-base materials including castor seed oil [9], using Kaolin, CaO, and ZnO as catalyst, as well as Jatropha waste [15], using HZSM-5, Co/HZSM-5, and Ni/HZSM-5 as catalyst. The yields of bio-oil by the catalytic upgrading of lipid-base materials stays around 60.0% (wt.) [9, 15].

4.2.2 *Effect of catalyst-to-biomass ration on the yields of bio-oils*

Figures 11 and 12 illustrate the effect of catalyst-to-biomass ration on the yields of bio-oil by the upgrading of residual fat pyrolysis vapors/volatiles at 450 °C, 1.0 atm, 0.0, 5.0, 7.5, and 10.0% (wt.) Red Mud pellets activated with 1.0 M HCl, using a catalyst fixed bed reactor, using a semi-pilot scale two-stage reactor of 2.0 L, compared with similar studies in the literature [8-9, 15, 25, 28-29]. The results depicted in Figures 11 and 12 show that increasing the catalyst-to-biomass causes an increase in the production of bio-oil, since the Red Mud pellets activated with 1M HCl favored the formation of organic liquid products. On the other hand, the yields of coke, H_2O, and gas decrease with increasing catalyst-

 doi:10.20944/preprints202204.0017.v1

to-biomass, that is, with increasing bio-oil production. In this context, it is expected that the characteristics of the catalyst, such as types of active centers, strength and distribution of active sites, as well as the size and structure of pores, selectively increased the yield of the bio-oil [1-19, 21-23, 25-26, 28-29, 30-32, 34]. Furthermore, the high yield and final distribution of the products are strongly dependent on process variables including reaction temperature, pressure, reactor type, residence time and raw material composition [8-9, 15, 25, 28-29, 31]. Thus, the process variables chosen in this work may have optimized the production of bio-oil. In addition, it is observed that the highest yields occur in the beginning of reaction, since, at that moment, the primary cracking occurs, in which occurs the formation of oxygenated compounds (fatty acids, ketones and acrolein) resulting from the rupture of the C-O bond of the glycerides present in vegetable oils and/or animal fat [35-37, 39]. Then, in the middle to the end of the reaction, secondary cracking occurs by de-carbonylation and de-carboxylation reactions, making it possible the production of hydrocarbons [35-37, 39-47].

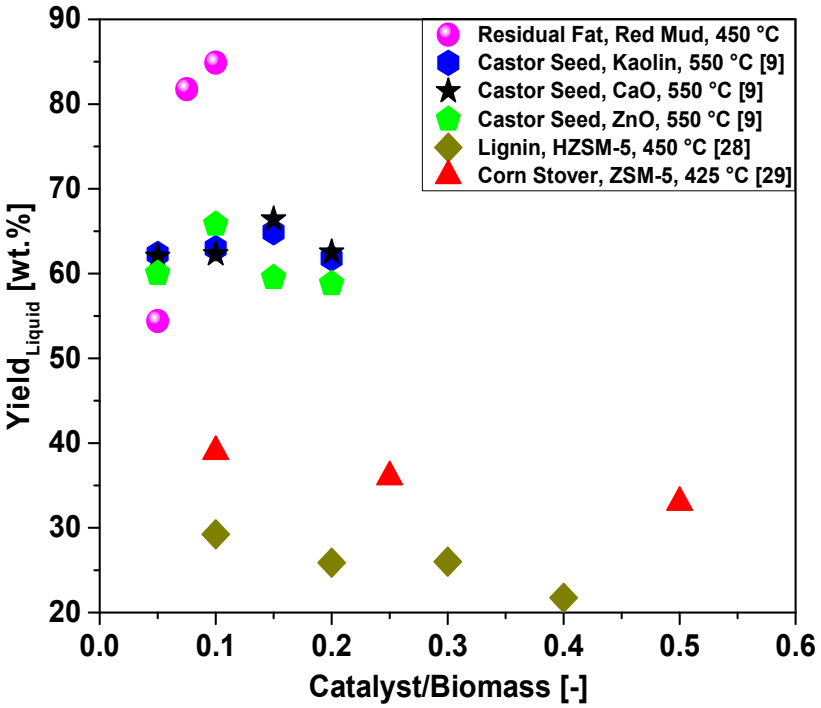

Figure 11. Effect of catalyst-to-biomass ratio within the range 0.0-0.5 on the yield of bio-oil by the upgrading of residual fat pyrolysis vapors at 450 °C, 1.0 atmosphere, 5.0, 7.5, and 10.0% (wt.) Red Mud pellets activated with 1.0 M HCl, using a catalyst fixed bed reactor, using a semi-pilot scale two-stage reactor of 2.0 L, compared with similar studies in the literature [9, 28-29].

By comparing the results illustrated in Figures 11 and 12, it has been observed sometimes that catalyst content limits the increase in bio-oil yield, so that after this limit, the yield of bio-oil decays, as shown in the literature by Koul *et. al.* [9], and Balasundram *et. al.* [25]. Koul *et. al.* [9], obtained the highest bio-oil yield with catalyst-to-biomass of 0.15 using Kaolin as catalyst and castor seed oil, while Balasundram *et. al.* [25], obtained the highest bio-oil yield with catalyst-to-biomass of 1.0 using HZSM-5 as catalyst and sugarcane bagasse. However, Balasundram *et. al.* [25], reported an increase of bio-oil yield with increasing catalyst-

Preprints (www.preprints.org) | NOT PEER-REVIEWED | Posted: 4 April 2022 doi:10.20944/preprints202204.0017.v1

to-biomass ratio in the range 0.5-2.0 using Ce/HZSM-5 as catalyst and sugarcane bagasse.

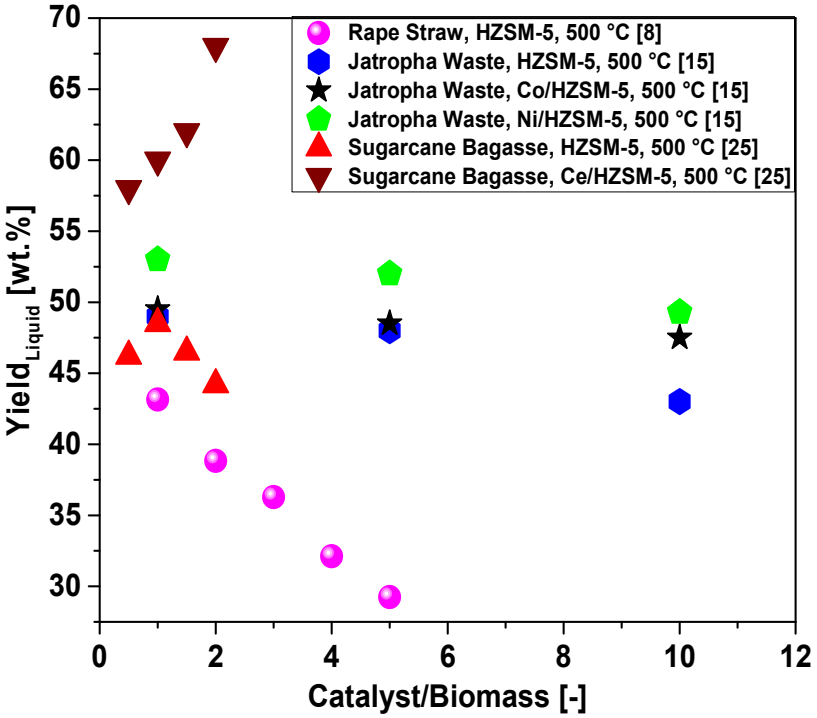

Figure 12. Effect of catalyst-to-biomass ratio within the range 0.5-10.0 on the yield of bio-oil by the upgrading of residual fat pyrolysis vapors at 450 °C, 1.0 atmosphere, 5.0, 7.5, and 10.0% (wt.) Red Mud pellets activated with 1.0 M HCl, using a catalyst fixed bed reactor, in a semi-pilot scale two-stage reactor of 2.0 L, compared with similar studies in the literature [8, 15, 25].

4.2.3 *Effect of reaction time on the yields of bio-oil and H_2O*

Table 3. Process parameters, mass balances, and partial yields of bio-oil and H_2O by residual fat pyrolysis at 450 °C, 1.0 atm, during the course of reaction at 50, 60, 70, and 80 min, using a semi-pilot reactor of 2.0 L.

Process Parameters	450 (°C)			
	0.00 (wt.)			
	50 (min)	60 (min)	70 (min)	80 (min)
Temperature of pyrolysis reactor (°C)	410	445	435	460
Temperature of fixed bed reactor (°C)	-	-	-	-
Mass of H_2O (g)	115	-	-	-
Yield of H_2O (wt.%)	11.5	-	-	-
Mass of Bio-oil (g)	294	311.98	176.1	12.15
Yield of Bio-oil (wt.%)	29.4	31.2	17.6	1.22

Tables 3, 4, 5, and 6 illustrate the process parameters, mass balances, and partial yields of bio-oil and H_2O by catalytic upgrading of residual fat pyrolysis vapors at 450 °C, 1.0 atm, 0.0, 5.0, 7.5, and 10.0% (wt.) Red Mud pellets activate with 1.0 M HCl, during the course of reaction at 40, 50, 60, 70, and 80 min, using a catalyst fixed bed reactor, in semi pilot scale two-stage reactor of 2.0 L.

 doi:10.20944/preprints202204.0017.v1

Table 4. Process parameters, mass balances, and partial yields of bio-oil and H_2O by catalytic upgrading of residual fat pyrolysis vapors at 450 °C, 1.0 atm, 5.0% (wt.) Red Mud pellets activated with 1.0 M HCl, using a catalyst fixed bed reactor, in a semi-pilot scale two-stage reactor of 2.0 L.

Process Parameters	450 (°C)			
	5.00 (wt.)			
	40 (min)	50 (min)	60 (min)	70 (min)
Temperature of pyrolysis reactor (°C)	400	417	440	450
Temperature of fixed bed reactor (°C)	380	365	405	462
Mass of H_2O (g)	19.63	-	-	-
Yield of H_2O (wt.%)	2.80	-	-	-
Mass of Bio-oil (g)	160.37	109.71	99.71	11
Yield of Bio-oil (wt.%)	22.91	15.67	14.24	1.57

Table 5. Process parameters, mass balances, and partial yields of bio-oil and H_2O by catalytic upgrading of residual fat pyrolysis vapors at 450 °C, 1.0 atm, 7.5% (wt.) Red Mud pellets activated with 1.0 M HCl, using a catalyst fixed bed reactor, in a semi-pilot scale two-stage reactor of 2.0 L.

Process Parameters	450 (°C)			
	7.50 (wt.)			
	40 (min)	50 (min)	60 (min)	70 (min)
Temperature of pyrolysis reactor (°C)	374	393	410	450
Temperature of fixed bed reactor (°C)	371	397	465	470
Mass of H_2O (g)	10.45	7	-	-
Yield of H_2O (wt.%)	1.49	1	-	-
Mass of Bio-oil (g)	102.45	197.74	172.67	94.22
Yield of Bio-oil (wt.%)	14.64	28.25	24.67	13.46

Table 6. Process parameters, mass balances, and partial yields of bio-oil and H_2O by catalytic upgrading of residual fat pyrolysis vapors at 450 °C, 1.0 atm, 10.0% (wt.) Red Mud pellets activated with 1.0 M HCl, using a catalyst fixed bed reactor, in a semi-pilot scale two-stage reactor of 2.0 L.

Process Parameters	450 (°C)			
	10.0 (wt.)			
	50 (min)	60 (min)	70 (min)	80 (min)
Temperature of pyrolysis reactor (°C)	375	403	423	450
Temperature of fixed bed reactor (°C)	394	404	428	455
Mass of H_2O (g)	14.1	1.4	-	-
Yield of H_2O (wt.%)	2.01	0.2	-	-
Mass of Bio-oil (g)	133.86	262.95	113.12	84.2
Yield of Bio-oil (wt.%)	19.12	37.56	16.16	12.03

The results illustrated in Tables 3, 4, 5, and 6 show that at the beginning of reaction, residual water is collected, proving that residual fat still contains water, that is, pre-processing (heating, homogenization) and separation processes (dehydration, sieving) could not completely remove residual water. In addition, the highest partial yield of bio-oil is obtained at the second withdraw between 50 and 60 minutes. The experiments described in Tables 3, 4, 5, and 6 makes it

Preprints (www.preprints.org) | NOT PEER-REVIEWED | Posted: 4 April 2022 doi:10.20944/preprints202204.0017.v1

possible not only to investigate the behavior of process kinetics by the catalytic upgrading of residual fat pyrolysis vapors at 450 °C, 1.0 atm, 0.0, 5.0, 7.5, and 10.0% (wt.) Red Mud pellets activated with 1.0 M HCl, using a catalyst fixed bed reactor, in semi pilot scale two-stage reactor of 2.0 L, but also to study the effect of reaction time on the physicochemical properties (density, kinematic viscosity, and acidity) and chemical composition of bio-oil.

4.2.4 *Effect of reaction time on the physicochemical properties of bio-oil*

Table 7 illustrates the effect of reaction time on the physicochemical properties (density, kinematic viscosity, and acidity) of bio-oil by catalytic upgrading of residual fat pyrolysis vapors at 450 °C, 1.0 atm, 0.0, 5.0, 7.5, and 10.0% (wt.) Red Mud pellets activated with 1.0 M HCl, using a catalyst fixed bed reactor, in semi pilot scale two-stage reactor of 2.0 L. It might be observed that except the refractive index, all other physicochemical properties of bio-oils (density, kinematic viscosity, and acidity) decrease with increasing reaction time.

Table 7. Effect of reaction time on the physicochemical properties of bio-oil by catalytic upgrading of residual fat pyrolysis vapors at 450 °C, 1.0 atm, 0.0, 5.0, 7.5, and 10.0% (wt.) Red Mud pellets activated with 1.0 M HCl, using a catalyst fixed bed reactor, in a semi-pilot scale two-stage reactor of 2.0 L.

Temperature/Catalyst	$t_{Reaction}$ **[min]**	**Physicalchemistry properties**			
		ϱ [g/cm³]	I.A [mg KOH/g]	I. R [-]	ν [mm²/s]
450 °C	50	0.861	131.10	1.445	9.80
	60	0.849	42.72	1.458	6.90
	70	0.847	33.90	1.460	6.30
	80	0.841	31.64	1.445	5.52
450 °C, 5% Red Mud (wt.)	40	0.843	113.90	1.444	4.20
	50	0.840	11.25	1.458	3.96
	60	0.838	6.98	1.473	3.83
	70	0.813	1.13	1.439	3.24
450 °C, 7.5% Red Mud (wt.)	40	0.871	135.27	1.445	8.45
	50	0.857	124.41	1.451	8.39
	60	0.844	72.18	1.458	5.30
	70	0.841	8.83	1.442	4.46
450 °C, 10% Red Mud (wt.)	50	0.874	124.41	1.408	8.10
	60	0.853	92.09	1.409	7.78
	70	0.848	42.50	1.405	4.10
	80	0.829	26.49	1.407	2.80

4.2.4.1 *Effect of reaction time on the density of bio-oil*

Figure 13 illustrates the effect of reaction time on the density of bio-oil by catalytic upgrading of residual fat pyrolysis vapors at 450 °C, 1.0 atm, 0.0, 5.0, 7.5, and 10.0% (wt.) of Red Mud pellets activated with 1.0 M HCl, using a catalyst fixed bed reactor, in semi pilot scale two-stage reactor of 2.0 L. For all the experiments, the density of bio-oil decreases as the reaction time increases. The density data of bio-oils for the experiments with 0.0, 7.5, and 10.0% (wt.) Red Mud pellets activated with 1.0 M HCl were correlated with a first order exponential decay model, exhibiting *root-mean-square error* (r^2) between 0.965 and 0.988, while

 doi:10.20944/preprints202204.0017.v1

the experiment with 5.0% (wt.) Red Mud pellets activated with 1.0 M HCl was correlated with a 1st order linear equation, exhibiting *root-mean-square error* (r^2) of 0.966. In addition, except for the experiment without catalyst, holding the reaction time constant (τ = 60 min), the density decreases as the content of catalyst decreases, showing that filling the fixed bed reactor with 5.0% (wt.) Red Mud pellets activated with 1.0 M HCl leads probably to an optimum value.

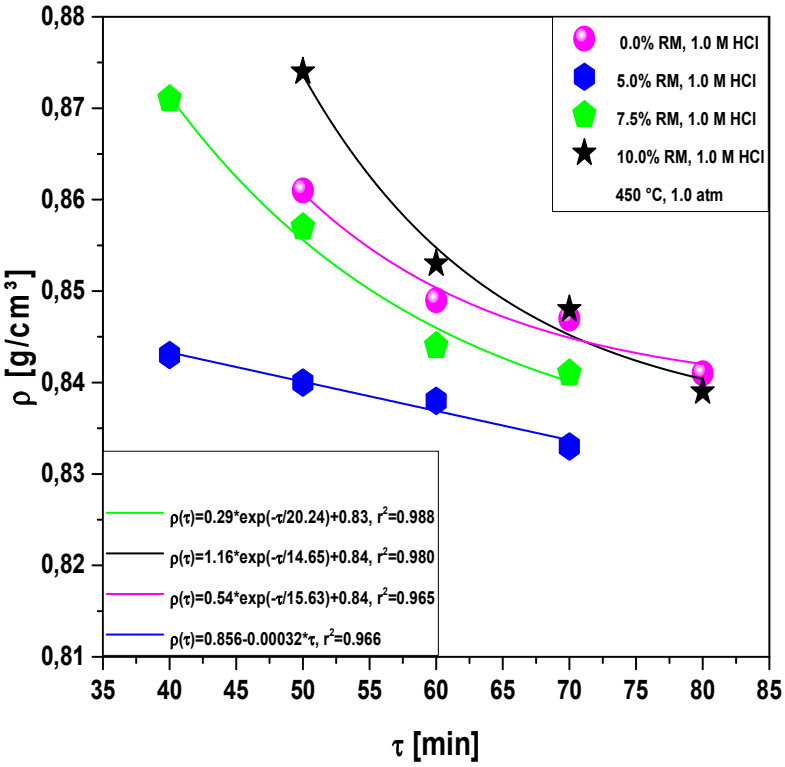

Figure 13. Effect of reaction time on the density of bio-oil by the upgrading of residual fat pyrolysis vapors at 450 °C, 1.0 atmosphere, 0.0, 5.0, 7.5, and 10.0% (wt.) Red Mud pellets activated with 1.0 M HCl, using a catalyst fixed bed reactor, using a semi-pilot scale two-stage reactor of 2.0 L.

4.2.4.2 *Effect of reaction time on the viscosity of bio-oil*

The effect of reaction time on the kinematic viscosity of bio-oil by catalytic upgrading of residual fat pyrolysis vapors at 450 °C, 1.0 atm, 0.0, 5.0, 7.5, and 10.0% (wt.) of Red Mud pellets activated with 1.0 M HCl, using a catalyst fixed bed reactor, in semi pilot scale two-stage reactor of 2.0 L, shown in Figure 14. For all the experiments, the kinematic viscosity of bio-oil decreases as the reaction time increases. The kinematic viscosity of bio-oils for the experiments with 7.5 and 10.0% (wt.) Red Mud pellets activated with 1.0 M HCl were correlated with a first order exponential model, exhibiting *root-mean-square error* (r^2) between 0.994 and 0.996, while the experiment with 5.0% (wt.) Red Mud pellets activated with 1.0 M HCl was correlated with a 1st order linear equation, exhibiting *root-mean-square error* (r^2) of 0.906. For the experiment without catalyst, the kinematic viscosity was correlated with a first order exponential model, exhibiting *root-mean-square error* (r^2) of 0.989. In addition, except for the experiment without catalyst, holding the reaction time constant (τ = 60 min), the kinematic viscosity decreases as the content of catalyst decreases. In fact, it is to expect the

kinematic viscosity to decrease as the reaction time succeeds, since at the beginning, the primary cracking occurs, forming oxygenated compounds (fatty acids, ketones and acrolein) [35-37, 39]. Then, in the middle to the end of the reaction, secondary cracking occurs by de-carbonylation and de-carboxylation reactions, producing hydrocarbons [35-37, 39-47], and hydrocarbons have much lower viscosity than oxygenates.

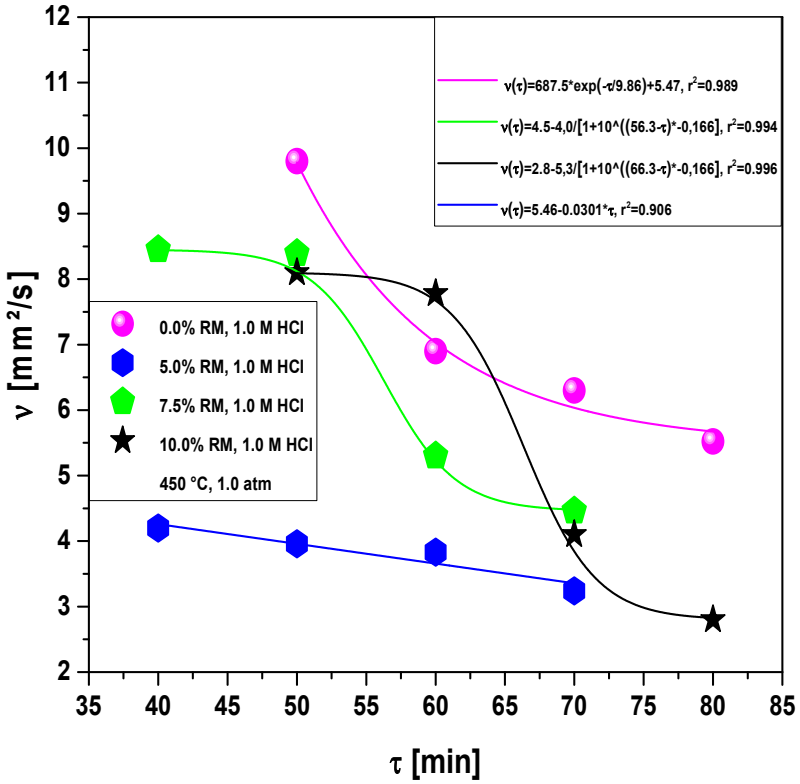

Figure 14. Effect of reaction time on the kinematic viscosity of bio-oil by the upgrading of residual fat pyrolysis vapors at 450 °C, 1.0 atmosphere, 0.0, 5.0, 7.5, and 10.0% (wt.) of Red Mud pellets activated with 1.0 M HCl, using a catalyst fixed bed reactor, using a semi-pilot scale two-stage reactor of 2.0 L.

4.2.4.3 *Effect of reaction time on the acidity of bio-oil*

Figure 15 shows the influence of reaction time on the density of bio-oil by catalytic upgrading of residual fat pyrolysis vapors at 450 °C, 1.0 atm, 0.0, 5.0, 7.5, and 10.0% (wt.) of Red Mud pellets activated with 1.0 M HCl, using a catalyst fixed bed reactor, in semi pilot scale two-stage reactor of 2.0 L. For all the experiments, the acidity of bio-oil, expressed by the acid value, decreases drastically as the reaction time succeeds. The experiments without catalyst and with 5.0% (wt.) Red Mud pellets activated with 1.0 M HCl were correlated with a *first order exponential decay model*, exhibiting *root-mean-square error* (r^2) of 0.999 and 0.998, respectively, while the experiments with 7.5 and 10.0% (wt.) Red Mud pellets activated with 1.0 M HCl were correlated with a *DoseResp* function, exhibiting root-mean-square errors (r^2) of 0.992 and 0.966, respectively. By DoseResp function, A1 and A2 are the bottom (initial value) and top (final value) asymptotes, respectively, being A1 equal to 8.8 and A2 equal to 135.2 for the experiment with 7.5% (wt.) Red Mud pellets activated with 1.0 M HCl, and A1 equal to 26.5 and

 doi:10.20944/preprints202204.0017.v1

A2 equal to 124.4 for the experiment with 10.0% (wt.) Red Mud pellets activated with 1.0 M HCl. In addition, except for the experiment without catalyst, holding the reaction time constant (τ = 60 min), the acid value decreases as the content of catalyst diminishes, showing that the catalyst fixed bed filled with 5.0% (wt.) Red Mud pellets activated with 1.0 M HCl proves to be can optimum value. This is due to the catalytic deoxygenation of triglycerides and fatty acids molecules, the main compounds of vegetable oils and animal fats, into hydrocarbons through de-carboxylation/de-carbonylation as reported in the literature [55-56].

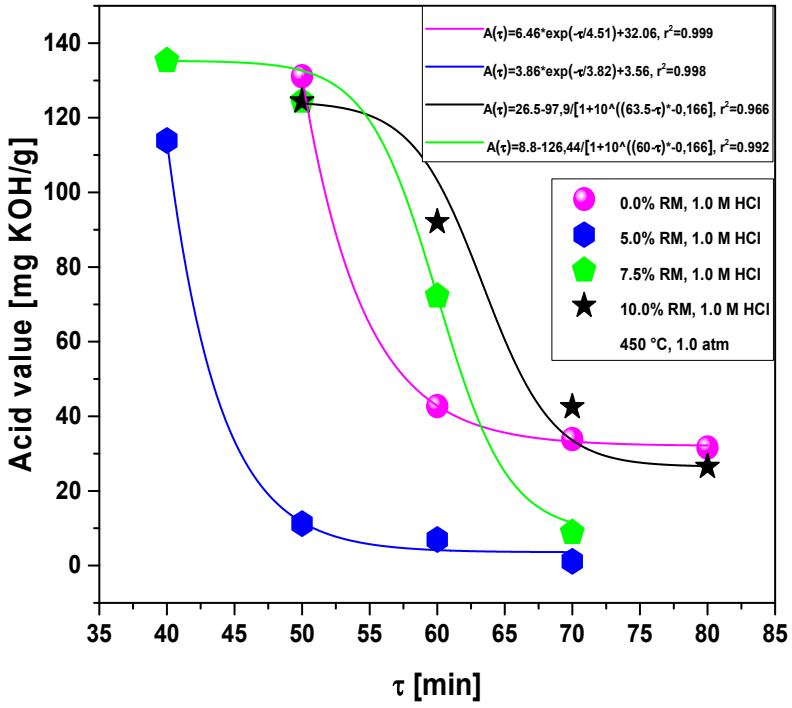

Figure 15. Effect of reaction time on the acidity of bio-oil by the upgrading of residual fat pyrolysis vapors at 450 °C, 1.0 atmosphere, 0.0, 5.0, 7.5, and 10.0% (wt.) of Red Mud pellets activated with 1.0 M HCl, using a catalyst fixed bed reactor, using a semi-pilot scale two-stage reactor of 2.0 L.

As observed in Figure 15, as soon as the first sample is withdrawn, the acid value is high, ranging between 135.3 and 113.9 mg KOH/g, due to formation of carboxylic acids, associated to the primary cracking. Afterwards, in the middle to the end of the reaction, deoxygenation of triglycerides and fatty acids molecules occurs by means of de-carboxylation/de-carbonylation, producing mixtures rich in hydrocarbons and poor of oxygenates, particularly carboxylic acids [55-56].

4.2.5 *Effect of reaction time on the content of hydrocarbons and oxygenates in bio-oil*

Table 8 and Figures 16 and 17 illustrate the effect of reaction time on the content of hydrocarbons and oxygenates, respectively, by the upgrading of residual fat pyrolysis vapors at 450 °C, 1.0 atmosphere, 0.0, 5.0, 7.5, and 10.0% (wt.) Red Mud pellets activated with 1.0 M HCl, using a catalyst fixed bed reactor, using a semi-pilot scale two-stage reactor of 2.0 L.

The chemical functions (alkanes, alkenes, aromatics, esters, carboxylic acids, furans, phenols, aldehydes, alcohols, and ketones), sum of peak areas, CAS

 doi:10.20944/preprints202204.0017.v1

numbers, and retention times of all the molecules identified in bio-oil by GC-MS by the upgrading of residual fat pyrolysis vapors at 450 °C, 1.0 atmosphere, 0.0, 5.0, 7.5, and 10.0% (wt.) Red Mud pellets activated with 1.0 M HCl, during the course of reaction at 40, 50, 60, 70, and 80 min, using a catalyst fixed bed reactor, using a semi-pilot scale two-stage reactor of 2.0 L, are illustrated in Supplementary Tables S9-S24.

Table 8. Effect of reaction time on the concentration of bio-oil by catalytic upgrading of residual fat pyrolysis vapors at 450 °C, 1.0 atm, 0.0, 5.0, 7.5, and 10.0% (wt.) Red Mud pellets activated with 1.0 M HCl, using a catalyst fixed bed reactor, in a semi-pilot scale two-stage reactor of 2.0 L.

Temperature/Catalyst	**$t_{Reaction}$ [min]**	**Concentration [%area.]**	
		Hydrocarbons	**Oxygenates**
450 °C	50	54.502	45.498
	60	58.523	41.477
	70	72.834	27.166
	80	77.944	22.056
450 °C, 5% Red Mud (wt.)	40	65.827	34.173
	50	90.203	9.797
	60	93.768	6.232
	70	95.347	4.653
450 °C, 7.5% Red Mud (wt.)	40	33.872	66.128
	50	41.103	58.897
	60	42.845	57.155
	70	94.324	5.676
450 °C, 10% Red Mud (wt.)	50	31.543	68.457
	60	49.631	50.369
	70	76.911	23.089
	80	83.104	16.896

 doi:10.20944/preprints202204.0017.v1

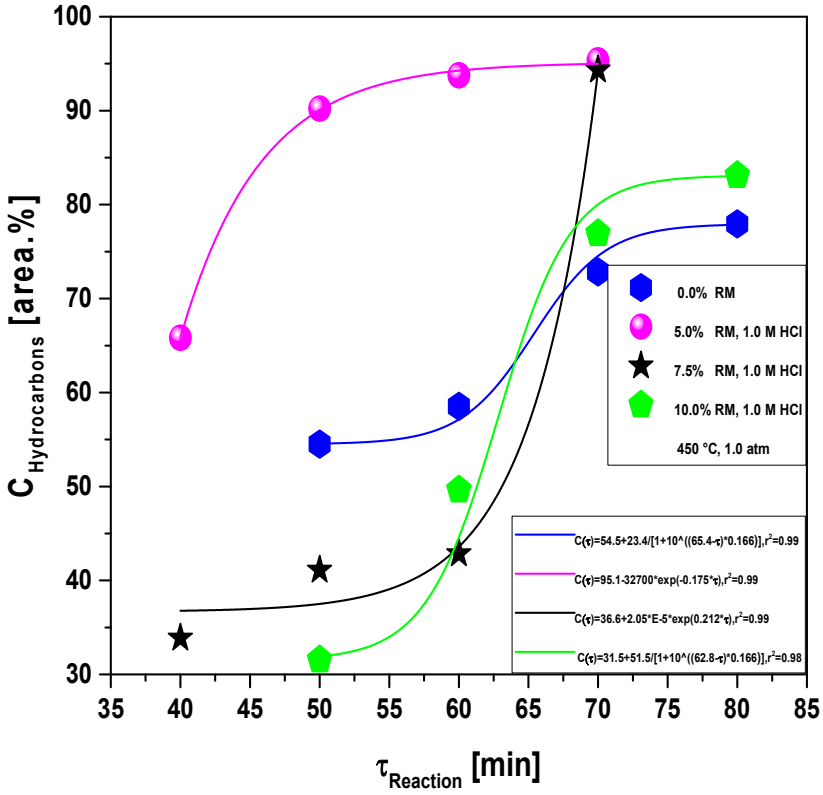

Figure 16. Effect of reaction time on the content of hydrocarbons by the upgrading of residual fat pyrolysis vapors at 450 °C, 1.0 atmosphere, 0.0, 5.0, 7.5, and 10.0% (wt.) Red Mud pellets activated with 1.0 M HCl, using a catalyst fixed bed reactor, using a semi-pilot scale two-stage reactor of 2.0 L.

For all the experiments, the concentration of hydrocarbons in bio-oil increases sharply with reaction time. The experiments without catalyst and with 10.0% (wt.) Red Mud pellets activated with 1.0 M HCl were correlated were correlated with a *DoseResp* function, exhibiting root-mean-square errors (r^2) of 0.99 and 0.98, respectively, while the experiments with 5.0 and 7.5% (wt.) Red Mud pellets activated with 1.0 M HCl were correlated with a *first order exponential growth model*, exhibiting *root-mean-square error* (r^2) of 0.99 and 0.99, respectively. The concentration of hydrocarbons in bio-oil increases due to the catalytic deoxygenation of fatty acids molecules, by means of de-carboxylation/de-carbonylation, producing aliphatic and aromatic hydrocarbons, as reported in the literature [55-56]. On the contrary, for all the experiments, the concentration of oxygenates in bio-oil decreases sharply as the reaction time increases The experiments without catalyst and with 10.0% (wt.) Red Mud pellets activated with 1.0 M HCl were correlated with a *DoseResp* function, exhibiting root-mean-square errors (r^2) of 0.99 and 0.98, respectively, while the experiments with 5.0 and 7.5% (wt.) Red Mud pellets activated with 1.0 M HCl were correlated with a *first order exponential growth model*, exhibiting *root-mean-square error* (r^2) of 0.99 and 0.99, respectively.

 doi:10.20944/preprints202204.0017.v1

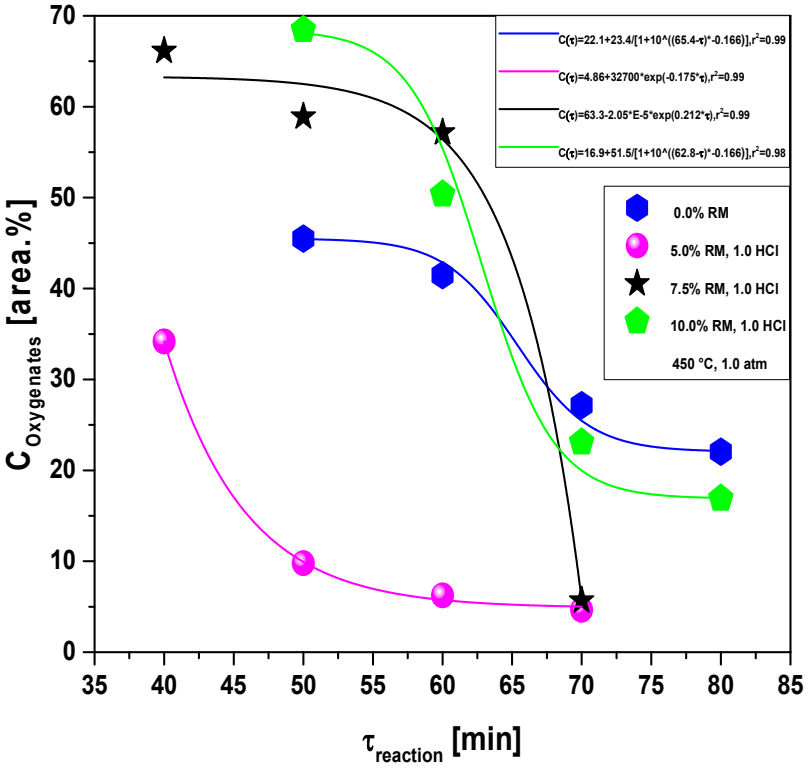

Figure 17. Effect of reaction time on the content of oxygenates by the upgrading of residual fat pyrolysis vapors at 450 °C, 1.0 atmosphere, 0.0, 5.0, 7.5, and 10.0% (wt.) Red Mud pellets activated with 1.0 M HCl, using a catalyst fixed bed reactor, using a semi-pilot scale two-stage reactor of 2.0 L.

5. Conclusions

The Red Mud pellets activated with 1.0 M HCl proved to be very efficient for the deoxygenation of triglycerides and fatty acids molecules by means of decarboxylation/de-carbonylation, producing mixtures rich in hydrocarbons and poor of oxygenates.

The catalytic upgrading experiments of residual fat pyrolysis vapors at 450 °C, 1.0 atm, 5.0% (wt.) Red Mud pellets activated with 1.0 M HCl, using a catalyst fixed bed reactor, using a semi-pilot scale two-stage reactor of 2.0 L, could achieve hydrocarbon concentrations up to 95.35% (area.).

Supplementary Materials: The following are available. Table ST9: Classes of compounds, summation of peak areas, CAS number, and retention times of chemical compounds identified by CG-MS in bio-oil by pyrolysis of residual fat at 450 °C, 1.0 atm, 50 min, using a pyrolysis reactor of 2.0 L, in semi pilot scale. Table ST10: Classes of compounds, summation of peak areas, CAS number, and retention times of chemical compounds identified by CG-MS in bio-oil by pyrolysis of residual fat at 450 °C, 1.0 atm, 60 min, using a pyrolysis reactor of 2.0 L, in semi pilot scale. Table ST 11: Classes of compounds, summation of peak areas, CAS number, and retention times of chemical compounds identified by CG-MS in bio-oil by pyrolysis of residual fat at 450 °C, 1.0 atm, 70 min, using a pyrolysis reactor of 2.0 L, in semi pilot scale. Table ST 12: Classes of compounds, summation of peak areas, CAS number, and retention times of chemical compounds identified by CG-MS in bio-oil by pyrolysis of residual fat at 450 °C, 1.0 atm, 80 min, using a pyrolysis

reactor of 2.0 L, in semi pilot scale. Table ST 13: Classes of compounds, summation of peak areas, CAS number, and retention times of chemical compounds identified by CG-MS in bio-oil by catalytic upgrading of residual fat pyrolysis vapors at 450 °C, 1.0 atm, 5.0% (wt.) Red Mud pellets activated with 1.0 M HCl, 40 min, using a catalyst fixed bed reactor, in semi pilot scale two-stage reactor of 2.0 L. Table ST 14: Classes of compounds, summation of peak areas, CAS number, and retention times of chemical compounds identified by CG-MS in bio-oil by catalytic upgrading of residual fat pyrolysis vapors at 450 °C, 1.0 atm, 5.0% (wt.) Red Mud pellets activated with 1.0 M HCl, 50 min, using a catalyst fixed bed reactor, in semi pilot scale two-stage reactor of 2.0 L. Table ST 15: Classes of compounds, summation of peak areas, CAS number, and retention times of chemical compounds identified by CG-MS in bio-oil by catalytic upgrading of residual fat pyrolysis vapors at 450 °C, 1.0 atm, 5.0% (wt.) Red Mud pellets activated with 1.0 M HCl, 60 min, using a catalyst fixed bed reactor, in semi pilot scale two-stage reactor of 2.0 L. Table ST 16: Classes of compounds, summation of peak areas, CAS number, and retention times of chemical compounds identified by CG-MS in bio-oil by catalytic upgrading of residual fat pyrolysis vapors at 450 °C, 1.0 atm, 5.0% (wt.) Red Mud pellets activated with 1.0 M HCl, 70 min, using a catalyst fixed bed reactor, in semi pilot scale two-stage reactor of 2.0 L. Table ST 17: Classes of compounds, summation of peak areas, CAS number, and retention times of chemical compounds identified by CG-MS in bio-oil by catalytic upgrading of residual fat pyrolysis vapors at 450 °C, 1.0 atm, 7.5% (wt.) Red Mud pellets activated with 1.0 M HCl, 40 min, using a catalyst fixed bed reactor, in semi pilot scale two-stage reactor of 2.0 L. Table ST 18: Classes of compounds, summation of peak areas, CAS number, and retention times of chemical compounds identified by CG-MS in bio-oil by catalytic upgrading of residual fat pyrolysis vapors at 450 °C, 1.0 atm, 7.5% (wt.) Red Mud pellets activated with 1.0 M HCl, 50 min, using a catalyst fixed bed reactor, in semi pilot scale two-stage reactor of 2.0 L. Table ST 19: Classes of compounds, summation of peak areas, CAS number, and retention times of chemical compounds identified by CG-MS in bio-oil by catalytic upgrading of residual fat pyrolysis vapors at 450 °C, 1.0 atm, 7.5% (wt.) Red Mud pellets activated with 1.0 M HCl, 60 min, using a catalyst fixed bed reactor, in semi pilot scale two-stage reactor of 2.0 L. Table ST 20: Classes of compounds, summation of peak areas, CAS number, and retention times of chemical compounds identified by CG-MS in bio-oil by catalytic upgrading of residual fat pyrolysis vapors at 450 °C, 1.0 atm, 7.5% (wt.) Red Mud pellets activated with 1.0 M HCl, 70 min, using a catalyst fixed bed reactor, in semi pilot scale two-stage reactor of 2.0 L. Table ST 21: Classes of compounds, summation of peak areas, CAS number, and retention times of chemical compounds identified by CG-MS in bio-oil by catalytic upgrading of residual fat pyrolysis vapors at 450 °C, 1.0 atm, 10.0% (wt.) Red Mud pellets activated with 1.0 M HCl, 50 min, using a catalyst fixed bed reactor, in semi pilot scale two-stage reactor of 2.0 L. Table ST 22: Classes of compounds, summation of peak areas, CAS number, and retention times of chemical compounds identified by CG-MS in bio-oil by catalytic upgrading of residual fat pyrolysis vapors at 450 °C, 1.0 atm, 10.0% (wt.) Red Mud pellets activated with 1.0 M HCl, 60 min, using a catalyst fixed bed reactor, in semi pilot scale two-stage reactor of 2.0 L. Table ST 23: Classes of compounds, summation of peak areas, CAS number, and retention times of chemical compounds identified by CG-MS in bio-oil by catalytic upgrading of residual fat pyrolysis vapors at 450 °C, 1.0 atm, 10.0% (wt.) Red Mud pellets activated with 1.0 M HCl, 70 min, using a catalyst fixed bed reactor, in semi pilot scale two-stage reactor of 2.0 L. Table ST 24: Classes of compounds, summation of peak areas, CAS number, and retention times of chemical compounds identified by CG-MS in in bio-oil by catalytic upgrading of residual fat pyrolysis vapors at 450 °C, 1.0 atm, 10.0% (wt.) Red Mud pellets activated with 1.0 M HCl, 80 min, using a catalyst fixed bed reactor, in semi pilot scale two-stage reactor of 2.0 L.

Author Contributions: The individual contributions of all the co-authors are provided as follows: C.C.F. contributed with formal analysis and writing original draft preparation, investigation and methodology, L.P.B. contributed with formal analysis and writing original draft preparation, investigation and methodology, A.F.d.F.C. contributed with formal analysis and writing original draft preparation, H.J.d.S.R. contributed with investigation and methodology, N.L.M. contributed with chemical analysis, Y.S.C. contributed with chemical analysis, A.C.F.B. contributed with chemical analysis, S.A.P.d.M. contributed with chemical analysis and formal analysis, C.C.V.Q. contributed with chemical

analysis, D.A.R.d.C. contributed with investigation and methodology, M.C.S. contributed with formal analysis, investigation and methodology, N.M.M. contributed with formal analysis, investigation and methodology, S.D.J. contributed with resources, chemical analysis, L.E.P.B. with co-supervision, and resources, and N.T.M. contributed with supervision, conceptualization, and data curation. All authors have read and agreed to the published version of the manuscript.

Funding: This research received no external funding.

Institutional Review Board Statement: Not applicable.

Informed Consent Statement: Not applicable.

Acknowledgments: I would like to acknowledge and dedicate this research in memory to Hélio da Silva Almeida, he used to work at the Faculty of Sanitary and Environmental Engineering/UFPa, and passed away on 13 March 2021. His contagious joy, dedication, intelligence, honesty, seriousness, and kindness will always be remembered in our hearts.

Conflicts of Interest: The authors declare no conflict of interest.

References

1. Qiang Lu, Ying Zhang, Zhe Tang, Wen-zhi Li, Xi-feng Zhu. Catalytic upgrading of biomass fast pyrolysis vapors with titania and zirconia/titania based catalysts. Fuel 89 (2010) 2096–2103
2. Guanlong Li, Lunjing Yan, Ruifang Zhao, Fan Li. Improving aromatic hydrocarbons yield from coal pyrolysis volatile products over HZSM-5 and Mo-modified HZSM-5. Fuel 130 (2014) 154–159
3. Xue-Yu Ren, Jing-Pei Cao, Xiao-Yan Zhao, Zhen Yang, Tian-Long Liu, Xing Fan, Yun-Peng Zhao, Xian-Yong Wei. Catalytic upgrading of pyrolysis vapors from lignite over mono/bimetalloaded mesoporous HZSM-5. Fuel 218 (2018) 33–40
4. Tian-Long Liu, Jing-Pei Cao, Xiao-Yan Zhao, Jing-Xian Wang, Xue-Yu Ren, Xing Fan, Yun-Peng Zhao, Xian-Yong Wei. In situ upgrading of Shengli lignite pyrolysis vapors over metal-loaded HZSM-5 catalyst. Fuel Processing Technology 160 (2017) 19–26
5. Lun-Jing Yan, Xiao-Jun Kong, Rui-Fang Zhao, Fan Li, Ke-Chang Xie. Catalytic upgrading of gaseous tars over zeolite catalysts during coal pyrolysis. Fuel Processing Technology 138 (2015) 424–429
6. Zhen Yang, Jing-Pei Cao, Xue-Yu Ren, Xiao-Yan Zhao, Sheng-Nan Liu, Zhen-Xing Guo, Wen-Zhong Shen, Jin Bai, Xian-Yong Wei. Preparation of hierarchical HZSM-5 based sulfated zirconium solid acid catalyst for catalytic upgrading of pyrolysis vapors from lignite pyrolysis. Fuel 237 (2019) 1079–1085
7. Elif Yaman, Adife Seyda Yargic, Nurgul Ozbay, Basak Burcu Uzun, Konstantinos G. Kalogiannis, Stylianos D. Stefanidis, Eleni P. Pachatouridou, Eleni F. Iliopoulou, Angelos A. Lappas. Catalytic upgrading of pyrolysis vapours: Effect of catalyst support and metal type on phenolic content of bio-oil. Journal of Cleaner Production 185 (2018) 52-61
8. Yongsheng Fan, Yixi Cai, Xiaohua Li, Ning Yu, Haiyun Yin. Catalytic upgrading of pyrolytic vapors from the vacuum pyrolysis of rape straw over nanocrystalline HZSM-5 zeolite in a two-stage fixed-bed reactor. Journal of Analytical and Applied Pyrolysis 108 (2014) 185–195
9. Mithelesh Koul, Krushna Prasad Shadangi, Kaustubha Mohanty. Effect of catalytic vapour cracking on fuel properties and composition of castor seed pyrolytic oil. Journal of Analytical and Applied Pyrolysis 120 (2016) 103–109
10. Yunwu Zheng, Fei Wang, Xiaoqin Yang, Yuanbo Huang, Can Liu, Zhifeng Zheng, Jiyou Gu. Study on aromatics production via the catalytic pyrolysis vapor upgrading of biomass using metal-loaded modified H-ZSM-5. Journal of Analytical and Applied Pyrolysis 126 (2017) 169–179
11. Xue-Yu Ren, Jing-Pei Caoa, Xiao-Yan Zhao, Wen-Zhong Shen, Xian-Yong Wei. Increasing light aromatic products during upgrading of lignite pyrolysis vapor over Co-modified HZSM-5. Journal of Analytical and Applied Pyrolysis 130 (2018) 190–197
12. Yixi Cai, Yongsheng Fan, Xiaohua Li, Lei Chen, Jiajun Wang. Preparation of refined bio-oil by catalytic transformation of vapors derived from vacuum pyrolysis of rape straw over modified HZSM-5. Energy 102 (2016) 95-105
13. Shuping Zhang, Houlei Zhang, Xinzhi Liu, Shuguang Zhu, Linlin Hu, Qiong Zhang. Upgrading of bio-oil from catalytic pyrolysis of pretreated rice husk over Fe-modified ZSM-5 zeolite catalyst. Fuel Processing Technology 175 (2018) 17–25
14. E.F. Iliopoulou, S.D. Stefanidis, K.G. Kalogiannis, A. Delimitis, A.A. Lappas, K.S. Triantafyllidis. Catalytic upgrading of biomass pyrolysis vapors using transition metal-modified ZSM-5 zeolite. Applied Catalysis B: Environmental 127 (2012) 281–290
15. Supawan Vichaphund, Duangdao Aht-ong, Viboon Sricharoenchaikul, Duangduen Atong. Catalytic upgrading pyrolysis vapors of Jatropha waste using metal promoted ZSM-5 catalysts: An analytical PY-GC/MS. Renewable Energy 65 (2014) 70-77

16. Xiaohua Li, Xiaolei Zhang, Shanshan Shao, Liangxiu Dong, Jin Zhang, Chao Hu, Yixi Cai. Catalytic upgrading of pyrolysis vapor from rape straw in a vacuum pyrolysis system over La/HZSM-5 with hierarchical structure. Bioresource Technology 259 (2018) 191–197
17. T.S. Nguyen, M. Zabeti, L. Lefferts, G. Brem, K. Seshan. Catalytic upgrading of biomass pyrolysis vapours using faujasite zeolite catalysts. Biomass and Bioenergy 48 (2013) 100-110
18. Kostas S. Triantafyllidis, Eleni F. Iliopoulou, Eleni V. Antonakou, Angelos A. Lappas, Hui Wang, Thomas J. Pinnavaia. Hydrothermally stable mesoporous aluminosilicates (MSU-S) assembled from zeolite seeds as catalysts for biomass pyrolysis. Microporous and Mesoporous Materials 99 (2007) 132–139
19. Xiaohua Li, Liangxiu Dong, Jin Zhang, Chao Hu, Xiaolei Zhang, Yixi Cai, Shanshan Shao. In-situ catalytic upgrading of biomass-derived vapors using HZSM-5 and MCM-41: Effects of mixing ratios on bio-oil preparation. Journal of the Energy Institute 92 (2019) 136-143
20. Ren, X. Y.; Feng, X. B.; Cao, J. P.; Tang, W.; Wang, Z. H.; Yang, Z.; Zhao, J. P.; Zhang, L. Y.; Wang, Y. J.; Zhao, X. Y. Catalytic conversion of coal and biomass volatiles: A review. Energy Fuels 2020, 34, 10307−10363
21. Calvin Mukarakate, Michael J. Watson, Jeroen ten Dam, Xavier Baucherel, Sridhar Budhi, Matthew M. Yung, Haoxi Ben, Kristiina Iisa, Robert M. Baldwin and Mark R. Nimlos. Upgrading biomass pyrolysis vapors over β-zeolites: role of silica-to-alumina ratio. Green Chem., 2014, 16, 4891–4905
22. Chaiwat Engtrakul, Calvin Mukarakate, Anne K. Starace, Kimberly A. Magrini, Allyson K. Rogers, Matthew M. Yung. Effect of ZSM-5 acidity on aromatic product selectivity during upgrading of pine pyrolysis vapors. Catalysis Today 269 (2016) 175–181
23. Xue-Yu Ren, Shi-Xuan Zhao, Jing-Pei Cao, Xiao-Yan Zhao, Xiao-Bo Feng, Yang Li, Ji Zhang, Zhi-Hao Wang, Hong-Cun Bai. Effect of coal ranks on light aromatics production during reforming of pyrolysis volatiles over HZSM-5 under Ar and H2-assisted atmospheres. Journal of Analytical and Applied Pyrolysis 152 (2020) 104958
24. Ofei D. Mante, Jose A. Rodriguez, Sanjaya D. Senanayake and Suresh P. Babu. Catalytic conversion of biomass pyrolysis vapors into hydrocarbon fuel precursors. Green Chem., 2015, 17, 2362–2368
25. Vekes Balasundram, Norazana Ibrahim, Rafiziana Md. Kasmani, Ruzinah Isha, Mohd. Kamaruddin Abd. Hamid, Hasrinah Hasbullah, Roshafima Rasit Ali. Catalytic upgrading of sugarcane bagasse pyrolysis vapours over rare earth metal (Ce) loaded HZSM-5: Effect of catalyst to biomass ratio on the organic compounds in pyrolysis oil. Applied Energy 220 (2018) 787–799
26. Umer Khalil, Jitaporn Vongsvivut, M. Shahabuddin, Shanthi Priya Samudrala, Srikanth Chakravartula Srivatsa, Sankar Bhattacharya. A study on the performance of coke resistive cerium modified zeolite Y catalyst for the pyrolysis of scrap tyres in a two-stage fixed bed reactor. Waste Management 102 (2020) 139–148
27. Nishu, Ronghou Liu, Md. Maksudur Rahman, Manobendro Sarker, Meiyun Chai, Chong Li, Junmeng Cai. A review on the catalytic pyrolysis of biomass for the bio-oil production with ZSM-5: Focus on structure. Fuel Processing Technology 199 (2020) 106301
28. Liangliang Fan, Paul Chen, Nan Zhou, Shiyu Liu, Yaning Zhang, Yuhuan Liu, Yunpu Wang, Muhammad Mubashar Omar, Peng, Min Addy, Yanling Cheng, Roger Ruan. In-situ and ex-situ catalytic upgrading of vapors from microwave-assisted pyrolysis of lignin. Bioresource Technology 247 (2018) 851–858
29. Nan Zhou, Shiyu Liu, Yaning Zhang, Liangliang Fan, Yanling Cheng, Yunpu Wang, Yuhuan Liu, Paul Chen, Roger Ruan. Silicon carbide foam supported ZSM-5 composite catalyst for microwaveassisted pyrolysis of biomass. Bioresource Technology 267 (2018) 257–264
30. Xue-Yu Ren, Jing-Pei Cao, Yang Li, Zi-Meng He, Xiao-Yan Zhao, Tian-Long Liu, Xiao-Bo Feng, Yun-Peng Zhao, Hong-Cun Bai, Ji Zhang, and Shi-Xuan Zhao. Formation of Light Aromatics and Coke during Catalytic Reforming of Biopolymer-Derived Volatiles over HZSM-5. Ind. Eng. Chem. Res. 2021, 60, 12521−12533
31. Changsong Hu, Rui Xiao, Huiyan Zhang. Ex-situ catalytic fast pyrolysis of biomass over HZSM-5 in a two-stage fluidized-bed/fixed-bed combination reactor. Bioresource Technology 243 (2017) 1133–1140
32. Peng Lv, Lunjing Yan, Yan Liu, Meijun Wang, Weiren Bao, and Fan Li. Catalytic Upgrading of Coal Pyrolysis Gaseous Tar over Hierarchical Y-Type Zeolites Synthesized Using a Microwave Hydrothermal Method. Ind. Eng. Chem. Res. 2019, 58, 21817−21826
33. Masoud Asadieraghi, Wan Mohd Ashri Wan Daud and Hazzim F. Abbas. Heterogeneous catalysts for advanced biofuel production through catalytic biomass pyrolysis vapor upgrading: a review. RSC Adv., 2015, 5, 22234–22255
34. Li-Yun Zhang, Jing-Pei Cao, Xue-Yu Ren, Xiao-Bo Feng, Jing-Xian Wang, Zi-Meng He, Tian-Long Liu, Zhen Yang, Xiao-Yan Zhao, and Hong-Cun Bai. Catalytic Upgrading of Cellulose Pyrolysis Volatiles over Ce Modified Hierarchical ZSM-5 Zeolite: Insight into the Effect of Acid Properties on Light Aromatics and Catalyst Stability. *Ind. Eng. Chem. Res. 2022, 61, 287−298*
35. H. da Silva Almeida, O.A. Corrêa, J.G. Eid, H.J. Ribeiro, D.A.R. de Castro, M.S. Pereira, L.M. Pereira, A. de Andrade Mâncio, M.C. Santos, J.A. da Silva Souza, Luiz E.P. Borges, N.M. Mendonça, N.T. Machado. Production of biofuels by thermal catalytic cracking of scum from grease traps in pilot scale. Journal of Analytical and Applied Pyrolysis 118 (2016) 20–33
36. H. da Silva Almeida, O.A. Corrêa, J.G. Eid, H.J. Ribeiro, D.A.R. de Castro, M.S. Pereira, L.M. Pereira, A. de Andrade Mâncio, M.C. Santos, S.A.P da Mota, J.A. da Silva Souza, Luiz E.P. Borges, N.M. Mendonça, N.T. Machado.

Performance of thermochemical conversion of fat, oils, and grease into kerosene-like hydrocarbons in different production scales. Journal of Analytical and Applied Pyrolysis 120 (2016) 126–143

37. H. da Silva Almeida, O.A. Corrêa, C.C. Ferreira, H.J. Ribeiro, D.A.R. de Castro, M.S. Pereira, A. de Andrade Mâncio, M.C. Santos, S.A.P. da Mota, J.A. da Silva Souza, Luiz E.P. Borges, N.M. Mendonça, N.T. Machado. Diesel-like hydrocarbon fuels by catalytic cracking of fat, oils, and grease (FOG) from grease traps. Journal of the Energy Institute 90 (2017) 337-354
38. Douglas Alberto Rocha de Castro, Haroldo Jorge da Silva Ribeiro, Lauro Henrique Hamoy Guerreiro, Lucas Pinto Bernar, Sami Jonatan Bremer, Marcelo Costa Santo, Hélio da Silva Almeida, Sergio Duvoisin, Jr., Luiz Eduardo Pizarro Borges, Nélio Teixeira Machado. Production of Fuel-Like Fractions by Fractional Distillation of Bio-Oil from Açaí (Euterpe oleracea Mart.) Seeds Pyrolysis. Energies 2021, 14, 3713
39. S.A.P. da Mota, A.A. Mancio, D.E.L. Lhamas, D.H. de Abreu, M.S. da Silva, W.G. dos Santos, D.A.R. de Castro, R.M. de Oliveira, M.E. Araújo, Luiz E.P. Borges, N.T. Machado. Production of green diesel by thermal catalytic cracking of crude palm oil (Elaeis guineensis Jacq) in a pilot plant. Journal of Analytical and Applied Pyrolysis 110 (2014) 1–11
40. Alisson Caio Magalhães Serrão, Conceição Maria Sales Silva, Fernanda Paula da Costa Assunção, Haroldo Jorge da Silva Ribeiro, Marcelo Costa Santos, Hélio da Silva Almeida, Sergio Duvoisin Jr., Luiz Eduardo Pizarro Borges, Douglas Alberto Rocha de Castro, Nélio Teixeira Machado. Process analysis of pyrolise of Açaí (Euterpe Oleracea, Mart) seeds: Influence of temperature on the yield of reaction products and physico-chemical properties of Bio-Oil. Brazilian Journal of Development, Curitiba, v.7, n.2, p. 18200-18220 feb. 2021
41. Mota, S. A. P., Mancio, A. A., Santanna, J. S., Gama, V. de J. P., & Machado, N. T. (2021). Influência do tempo de reação sobre as propriedades físico-químicas de biocombustíveis obtidos através do craqueamento térmico catalítico do óleo de palma bruto. *Scientia Plena*, *17*(6). https://doi.org/10.14808/sci.plena.2021.064201
42. Flávio Pinheiro Valois, Ana Rosa Bezarra Cardoso, Raymundo da Costa França Neto, Lia Martins Pereira, Dyenny Ellen Lima Lhamas, Sílvio Alex Pereira da Mota, Hélio da Silva Almeida, Luiz Eduardo Pizarro Borges, Nélio Teixeira Machado, Marcelo Costa Santos. Thermal catalytic cracking of soap phase residue of neutralization process of palm oil using $CaCO_3$ as catalyst. Brazilian Journal of Development, Curitiba, v.7, n.6, p.59461-59481jun.2021
43. Romero Moreira de Oliveira, Emerson Cardoso Rodrigues, Dilson Nazareno Pereira Cardoso, Wenderson Gomes dos Santos, Nélio Teixeira Machado. Thermocatalytic cracking of fat from fat boxes with activated red mud. Braz. J. of Develop.,Curitiba, v. 6, n.4,p.19876-19887apr.2020.ISSN 2525-8761
44. Lia Martins Pereira, Nélio Teixeira Machado, Hélio da Silva Almeida, Fernanda Paula da Costa Assunção, Laércio dos Santos Rosa Junior. Characterization of biocarvia through catalytic thermal cracking from blendof sewage and residual fat in scale pilot. Braz. J. of Develop.,Curitiba, v. 6, n. 1,p.1502-1509 jan. 2020. ISSN 2525-8761
45. A.A. Mancio, S.A.P. da Mota, C.C. Ferreira, T.U.S. Carvalho, O.S. Neto, J.R. Zamian, M.E. Araújo, L.E.P. Borges, N.T. Machado. Separation and characterization of biofuels in the jet fuel and diesel fuel ranges by fractional distillation of organic liquid products. Fuel 215 (2018) 212–225
46. A.A. Mâncio, K.M.B. da Costa, C.C. Ferreira, M.C. Santos, D.E.L. Lhamas, S.A.P. da Mota, R.A.C Leão, R.O.M.A. de Souza, M.E. Araújo, L.E.P. Borges, N.T. Machado. Process analysis of physicochemical properties and chemical composition of organic liquid products obtained by thermochemical conversion of palm oil. Journal of Analytical and Applied Pyrolysis 123 (2017) 284–295
47. M.C. Santos, R.M. Lourenço, D.H. de Abreu, A.M. Pereira, D.A.R. de Castro, M.S. Pereira, H.S. Almeida, A.A. Mâncio, D.E.L. Lhamas, S.A.P. da Mota, J.A. da Silva Souza, S.D. Júnior, M.E. Araújo, L.E.P. Borges, N.T. Machado. Gasoline-like hydrocarbons by catalytic cracking of soap phase residue of neutralization process of palm oil (Elaeis guineensis Jacq). Journal of the Taiwan Institute of Chemical Engineers 71 (2017) 106–119
48. Yongsheng Fan, Yonglian Xiong, Weidong Zhao, Lizhu Jin, and Yuwei Chen. Process optimization and stability characterization of the bio-oil produced from vacuum pyrolysis of rape straw. ENERGY SOURCES, PART A: RECOVERY, UTILIZATION, AND ENVIRONMENTAL EFFECTS 2021, VOL. 43, NO. 13, 1649–1659, https://doi.org/10.1080/15567036.2019.1663302
49. J.M. Rivas Mercury, I.L.G. Galdino, N.S.L.S. Vasconcelos, A.E.M. Paiva, A.A. Cabral, R.S. Angélica. Estudo do comportamento térmico e propriedades físico-mecânicas da lama vermelha, Rev. Matér. 15 (3) (2010) 445–460
50. Yanzhong Li, Changjun Liu, Zhaokun Luan, Xianjia Peng, Chunlei Zhu, Zhaoyang Chen, Zhongguo Zhang, Jinghua Fan, Zhiping Jia. Phosphate removal from aqueous solutions using raw and activated red mud and fly ash. Journal of Hazardous Materials B137 (2006) 374–383
51. Manoj Kumar Sahu, Sandip Mandal, Saswati S. Dash, Pranati Badhai, Raj Kishore Patel. Removal of Pb(II) from aqueous solution by acid activated red mud. Journal of Environmental Chemical Engineering 1 (2013) 1315–1324
52. Weiwei Huang, Shaobin Wang, Zhonghua Zhu, Li, Xiangdong Yao, Victor Rudolph, Fouad Haghseresht. Phosphate removal from wastewater using red mud. Journal of Hazardous Materials 158 (2008) 35–42
53. Liu Chang-jun, Li Yan-zhong, Luan Zhao-kun, Chen Zhao-yang, Zhang Zhong-guo, Jia Zhi-ping. Adsorption removal of phosphate from aqueous solution by active red mud. Journal of Environmental Sciences 19(2007) 1166–1170

 doi:10.20944/preprints202204.0017.v1

54. Estudo da Aplicação da Lama Vermelha como Catalisador na Reação de Craqueamento Térmico de Resíduos de Caixa de Gordura. Master Thesis, PPGEQ-UFPA, Janaína Guedes Aid, 2015.https://ppgeq.propesp.ufpa.br/ARQUIVOS/dissertacoes/Janaina%20Guedes%20Eid.pdf
55. Eduardo Santillan-Jimenez, Tonya Morgan, Joseph Lacny, Susanta Mohapatra, Mark Crocker. Catalytic deoxygenation of triglycerides and fatty acids to hydrocarbons over carbon-supported nickel. Fuel 103 (2013) 1010–1017
56. Hao Chena, Yulong Wub, Suitao Qi, Yu Chenb, Mingde Yang. Deoxygenation of octanoic acid catalyzed by hollow spherical Ni/ZrO_2. Applied Catalysis A: General 529 (2017) 79–90